TRANSIENT TWO-PHASE FLOW THROUGH POROUS MEDIA

Thasis for the Dogree of Ph. D.
MICHIGAN STATE UNIVERSITY
Kuang-ming Lin
1964



This is to certify that the

thesis entitled

Transient Two-Phase Flow Through Porous Media

presented by

Kuang-ming Lin

has been accepted towards fulfillment of the requirements for

<u>Ph.D</u> degree in <u>Mechani</u>cs

Date November 25, 1964

O-169

ROOM USE ONLY

ABSTRACT

TRANSIENT TWO-PHASE FLOW THROUGH POROUS MEDIA

by Kuang-ming Lin

This thesis presents an analytical investigation by which the movement of the interface for transient twophase flow through porous media can be determined. Two approaches, one-dimensional flow and two-dimensional flow, are considered in the analysis of the problem. one-dimensional flow, the governing equations are solved simply by a finite-difference method. It is found that the results are not very satisfactory near the outflow Therefore, two-dimensional flow is . seepage face. emphasized. The essential idea utilized in two-dimensional flow is to treat the interface as a distribution of sources and to apply the concept of Green's function to the governing differential equation in obtaining the solution. For purposes of illustration, a case of confined finite aguifer of rectangular shape is considered. The two interacting fluids are assumed incompressible and immiscible. A Control Data 3600 computer is used for all the numerical computation.

TRANSIENT TWO-PHASE FLOW

THROUGH

POROUS MEDIA

Ву

Kuang-ming Lin

A THESIS

Submitted to
Michigan State University
in partial fulfillment of the requirements
for the degree of

DOCTOR OF PHILOSOPHY

Department of Metallurgy, Mechanics, and Materials Science

ACKNOWLEDGEMENTS

The author wishes to express his gratitude to Dr. George E. Mase for his constant encouragement and advice throughout the author's graduate work at Michigan State University. Also, thanks are due Dr. Harold R. Henry for suggesting the subject of this dissertation and for his continuous quidance during its preparation. Dr. Lawrence E. Malvern, Dr. Joachim E. Lay, and Dr. J. Sutherland Frame are also to be thanked for their serving on the Guidance Committee and for reviewing this thesis. For the computational work of this thesis, the author is indebted to the Computer Center and its staff for their co-operation and generous allowance of the computer time which made the execution of the tremendous amount of computation in this thesis possible. Finally, the author would like to thank his wife, Pi-yau, for her patience and encouraging words during the entire period of his graduate study.

TABLE OF CONTENTS

																Page
ACKNOWL	EDGEMENT	s.	•		•	•		•	•	•	•	•	•	•	•	ii
LIST OF	TABLES		•		•	•	• •	•	•	•	•	•	•	•	•	iv
LIST OF	FIGURES		•		•	•	•	•	•	•	•	•	•	•	•	v
LIST OF	APPENDI	CES .	•		•	•	• •	•	•	•	•	•	•	•	•	vi
Chapter																
I.	INTRODU	CTION	1.		•	•	• •	•	•	•	•	•	•	•	•	1
	A. B. C.	Stat Gene Revi	eral	Th	eoi	-Y−	−Da	rcy	, ' s	s I	aw	<i>i</i> •	•	•	•	1 4 12
II.	ONE-DIM	ENSIC	NAL	AN	AL	ZSI	s.	•	•	•	•	•	•	•	•	15
	A. B. C.	Deri Nume Fini	eric	al	Exa	qme	le.	•	•	•	•				•	15 20
	D.	Proc	edu	re.	•	•		•	•	•	•	•	•	•	•	23 24
III.	TWO-DIM	ENSIC	NAL	, AN	AL	/SI	s.	•	•	•	•	•	•	•	•	34
	Α.	Form	lem	۱	۰	•		•	•	•	•	•	•	•	•	34
	B. C. D.	Solu Fund Nume Resu	tic eric	n .	Exa	amp	le.	•	•	•	•	•	•	•	•	40 45 46
IV.	CONCLUS	ION .	•		•	•	• •	•	•	•	•	•	•	•	•	62
BIBLIOG	RAPHY .	• • •	•		•	•	• •	•	•	•	•	•	•	•	•	64
APPENDI	CES															66

LIST OF TABLES

Table		Page
1.	Tabulation for Figures 5 and 6	31
2.	Tabulation for Figure 7	32
3.	Tabulation for Figure 8	33
4.	<pre>Values of PSI along Initial Interface for y/d = 0.1 to 0.8 (Tabulation for Figure 13)</pre>	52
5.	Movement of Interface PositionCase 4 (Tabulation for Figure 14)	54
6.	Values of PSI for Initial Interface Position y = 0.810 to 0.982 (Tabulation of Figure 15)	55
7.	Movement of Interface PositionCase 5 (Tabulation of Figure 16)	61

LIST OF FIGURES

Figure		Page
1.	Geometry of the Problem	2
2.	Generalized Darcy's Experiment	6
3.	Graph of Equation (1)	7
4.	Flow Geometry for One-dimensional Analysis	16
5.	Plot of h/d vs. x/d	27
6.	Movement of InterfaceCase 1	28
7.	Movement of InterfaceCase 2	29
8.	Movement of InterfaceCase 3	30
9.	Geometry of Flow and Boundary Conditions .	35
10.	Boundary Conditions in Terms of $\psi...$	39
11.	Boundary Conditions in Terms of $\Psi{ ext{.}}{ ext{.}}{ ext{.}}{ ext{.}}$	40
12.	Boundary Conditions for G	41
13.	Plot of Ψ' vs. y/d	48
14.	Movement of InterfaceCase 4	49
15.	ψ' vs. y/d	50
16.	Movement of InterfaceCase 5	51

LIST OF APPENDICES

Appendi	×	Page
I.	LIST OF SYMBOLS	66
II.	FORMULAS USED IN NUMERICAL APPROXIMATION .	68
	A. Newton's Divided-difference Interpolation Formula	68
	Numerical Integration	69
	Formulas	69
III.	FLOW CHART FOR COMPUTATION	70
IV.	SAMPLE FORTRAN PROGRAMS	72
	PROGRAM PSI	73 78
V.	GREEN'S FUNCTION FOR LAPLACE'S EQUATION AND POISSON'S EQUATION	79
	A. Definition	79
	Chapter III	83

CHAPTER I

INTRODUCTION

A. Statement of the Problem

The object of this thesis is to investigate analytically the unsteady flow patterns which exist in porous media when two adjacent fluids of different densities are in a non-equilibrium state. The primary consideration is given to the determination of the movement of the interface separating the fluids. The analytical treatment of such a problem is generally very difficult, and only a handful of solutions of special cases are available. Some of the more important of these with respect to this investigation are described in part C of this chapter and are also listed in the Bibliography. Practical engineering situations in which the results of this investigation may be applied occur in the problems of sea-water encroachment into fresh-water aquifers and in the area of petroleum recovery techniques.

In this thesis, the physical arrangement in which the problem is formulated consists of a rectangular porous medium, confined in the horizontal direction, together with two adjacent liquid reservoirs as indicated schematically by Figure 1. For the problems to be considered

the horizontal dimension of the rectangle is actually some twenty times the vertical dimension, so that the interfaces and the flow are much more nearly horizontal than they appear in Figure 1.

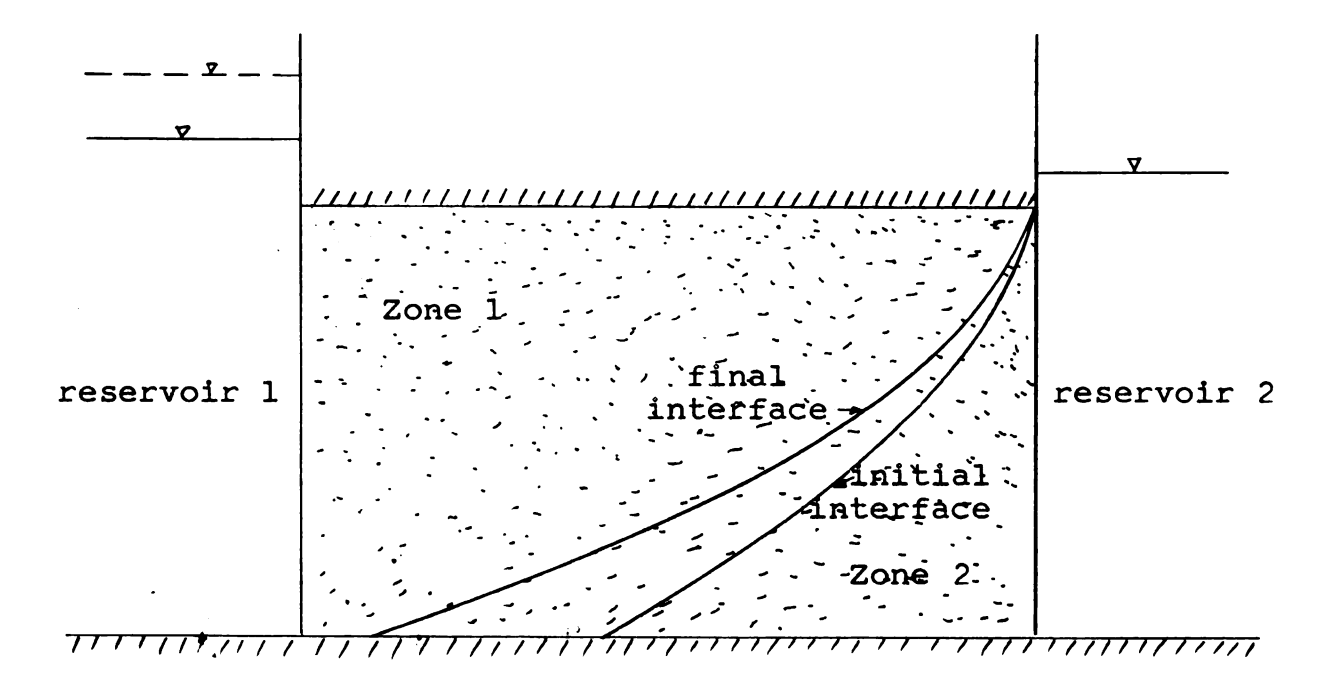


Figure 1.——Geometry of the Problem

When the piezometric head of one of the liquid reservoirs is suddenly changed by a certain amount and then kept at a constant value, the flow of liquid through the porous medium is unsteady and the interface moves toward a new equilibrium position. Such a condition is observed frequently in nature when a heavy rainfall occurs or during a drought when the heavy withdrawal of ground water supply takes place. It is the purpose of this thesis to apply an analytical treatment to the problem of the establishment of flow through a porous medium and especially the motion

of the interface under such conditions during the transient state.

Darcy's law is a fundamental law upon which the mathematical theory of flow through porous media is formulated. The investigation as reported herein analyzes the problem from two different assumptions, one-dimensional flow and two-dimensional flow. The former is presented in Chapter II and the latter in Chapter III. In the onedimensional analysis, the directions of the velocities are assumed to be in the x-direction only. Since the horizontal dimension is twenty times the vertical in Figure 1, this would seem to be a reasonable assumption over most of the region. The resulting governing differential equations are replaced by the corresponding finite-difference equations, and these are solved numerically. The results thus obtained show that this approach is not completely satisfactory, and the need for two-dimensional analysis is apparent. The inaccuracy of the one-dimensional approach stems from the fact that the velocities near the out-flow seepage face change their directions very rapidly, thus making the one-dimensional flow assumption invalid. The emphasis, therefore, will be placed on the twodimensional analysis, which describes more realistically the physical situation. The one-dimensional analysis is not totally without merit, however, since it does apply over the major part of the region and also serves as a quide to the two-dimensional analysis.

The essential idea employed in the two-dimensional analysis is to consider the interface as a distribution of sources and to apply the concept of a Green's function to the governing differential equations in obtaining a solution. The resulting solution is in the form of a double infinite series. With the aid of a modern high speed computer, such as the Control Data 3600 system at Michigan State University, sufficient convergence can be obtained in a reasonable amount of time to yield a solution within the range required by engineering accuracy.

B. General Theory--Darcy's Law

Flow through a porous medium, like any other type of flow, obeys Newton's second law of motion, which states that "forces must be exerted on a fluid to change either the direction or magnitude of the fluid velocity." When a fluid flows through a porous medium, the velocity of a fluid element changes rapidly from point to point along its tortuous flow path. The forces which produce these changes in velocity vary rapidly from point to point.

However, in a naturally porous material the porous structure and hence the multitude of flow paths have a random character. It is reasonable, therefore, to suppose that the random variations in flow patterns for any particular fluid element are uniformly distributed. Also the variations in magnitude of velocity can be expected to be distributed uniformly with mean zero. Thus, for steady laminar flow the lateral forces associated with the

microscopic random variations in velocity can be expected to average to zero over any macroscopic volume. However, the inertial forces in the direction of flow will not average to zero and hence will only be negligible for low flow rates. Fortunately, the flow in most cases of practical interest is of the slow laminar type and Darcy's law, which is presented below, applies. The mathematical theory of flow through porous media is always formulated with Darcy's law being taken as the fundamental law of flow.

In the middle of the 19th century, Henry Darcy, a French engineer, discovered through experiments a law governing the flow of water through filter beds. This law expressed in vectorial form is

$$\overrightarrow{q} = -grad \ \Phi^* \tag{1}$$

or

$$\overrightarrow{q} = -\nabla \varphi$$
.

In this equation, \overrightarrow{q} is the velocity vector,

$$\Phi = kh = k(\frac{p}{\gamma} + \gamma)$$
 (2)

is the velocity potential, and h is the piezometric head. For the meaning of $\frac{p}{\gamma}$ and y, refer to Figure 2. Here, the liquid of specific weight γ is flowing with a flow rate of Q (dimension L^3/T) through a tube which is filled with

^{*}A complete list of symbols with their definitions is given in Appendix I.

a porous medium of length L. It is seen that $\frac{p}{y}$ and y represent the pressure head and the elevation, respectively.

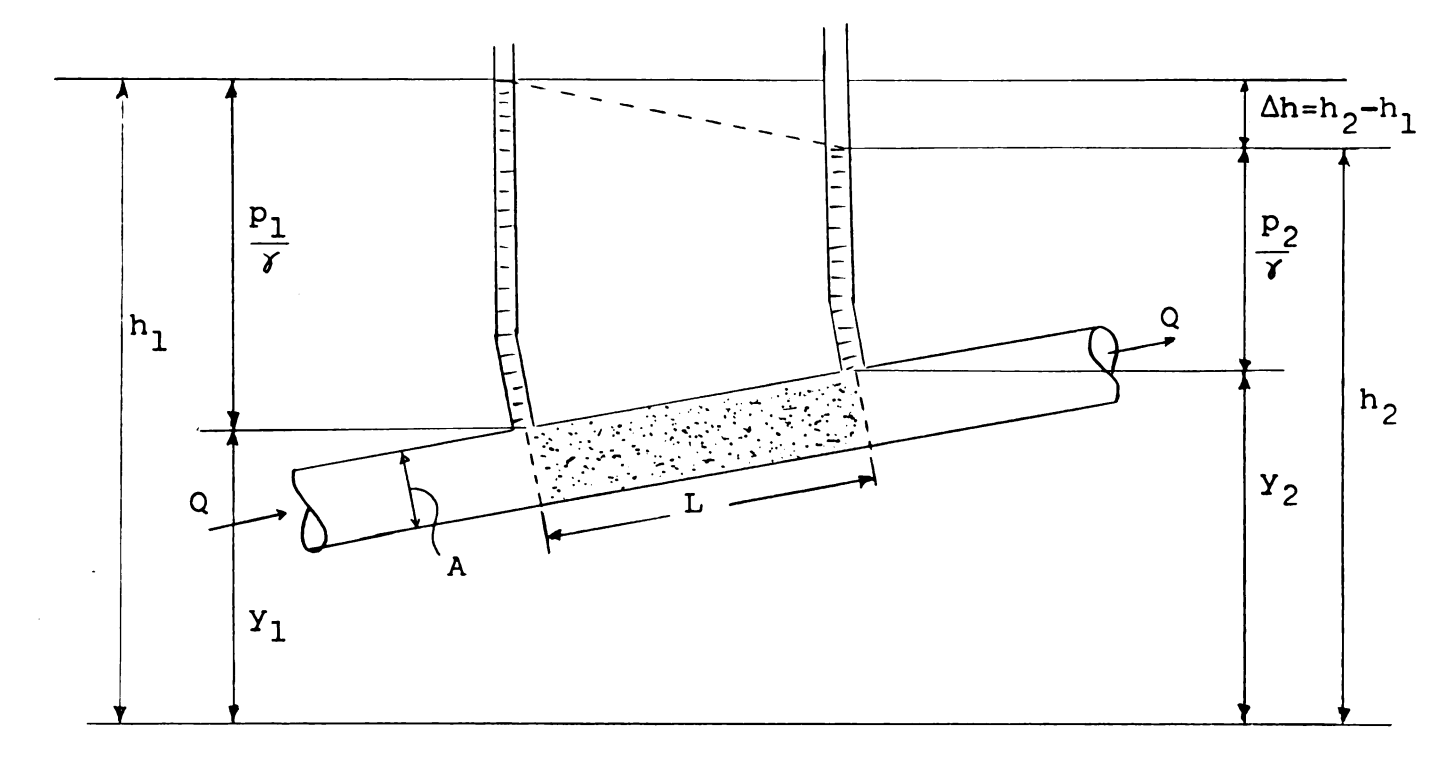


Figure 2.--Generalized Darcy's Experiment

From dimensional analysis, the hydraulic conductivity k can be expressed as

$$\mathbf{k} = \mathrm{cd}^2 \frac{\gamma}{\mu}. \tag{3}$$

The dimensionless factor c combines the effects of porosity, range and distribution of grain sizes, and shape of grains as well as their orientation and packing, while d, the mean grain size, is representative of the average pore size. The hydraulic conductivity k depends on the properties c and d of the medium as well as on the specific weight γ and viscosity μ of the fluid.

The product K = cd² is typical of the medium alone and is called the "permeability."

Darcy's law is invariant with respect to the direction of flow in the earth's gravitational field. This can be proved by the flow in the apparatus sketched in Figure 2. This property was not recognized immediately, since Darcy performed his experiment in a vertical pipe. Figure 3 illustrates the vector character of Equation (1) with the velocity potential of Equation (2) for the case where Y = P g is independent of position, as in a homogeneous incompressible fluid.

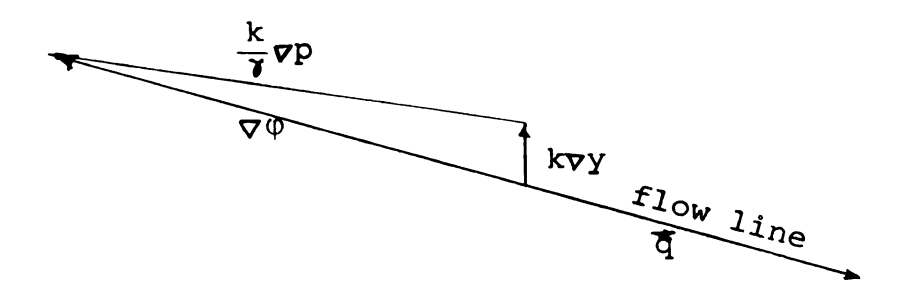


Figure 3.--Graph of Equation (1)

Since $g \neq y = -g\hat{j}$, where g is the acceleration of gravity and \hat{j} is a unit vector in the +y-direction, it follows from Equation (2) that for a homogeneous incompressible fluid

$$-\frac{q}{k} \operatorname{grad} \Phi = g\hat{j} - \frac{1}{\rho} \operatorname{grad} p. \tag{4}$$

Equation (4) states that the force exerted upon the unit mass of fluid at a point has a gravity component and a component caused by the gradient of fluid pressure. Thus, g_0 is a measure of the energy per unit mass or the potential of the fluid at any point of the system. The flow takes place from higher to lower energy levels. For horizontal flow this means that the flow takes place from higher to lower pressure, but this is not necessarily the case when the flow is not horizontal because of the gravitational potential.

Darcy's law states, in view of the above consideration, that macroscopically the velocity of the water flowing through the porous medium is proportional to the negative gradient of the piezometric head. The macroscopic velocity magnitude q is a bulk velocity smaller than the actual seepage velocity magnitude \mathbf{q}_{se} in the pores, to which it is simply related by the porosity $\boldsymbol{\theta}$ as

 $q = \theta q_{se}$

Although Darcy's law was first established by experiment, Hubbert (1956)*, and others, have derived it from the general Navier-Stokes equations for viscous flow. Such derivations stem from statistical considerations and

^{*}The number in the parentheses refers to the year of the publication. References are listed in the Bibliography at the end of the thesis.

Although they do not contribute to the formulation of a new law, they confirm the earlier belief that Darcy's law is of the nature of a statistical result giving the empirical equivalent of the Navier-Stokes equations. The Navier-Stokes equations for two-dimensional flow of incompressible fluid are:

$$\frac{\partial \mathbf{u}}{\partial \mathbf{t}} + \mathbf{u} \frac{\partial \mathbf{u}}{\partial \mathbf{x}} + \mathbf{v} \frac{\partial \mathbf{u}}{\partial \mathbf{y}} = -\frac{1}{\rho} \frac{\partial \mathbf{p}}{\partial \mathbf{x}} + \frac{\mathcal{U}}{\rho} \nabla^2 \mathbf{u}$$

$$\frac{\partial \mathbf{v}}{\partial t} + \mathbf{u} \frac{\partial \mathbf{v}}{\partial \mathbf{x}} + \mathbf{v} \frac{\partial \mathbf{v}}{\partial \mathbf{y}} = -\frac{1}{\rho} \frac{\partial \mathbf{p}}{\partial \mathbf{y}} + \frac{\mathcal{M}}{\rho} \nabla^2 \mathbf{v} - \mathbf{g}.$$

One can summarize the statistical averages by the approximate assumptions

$$\nabla^2 u = -c \frac{u}{L^2}$$
 and $\nabla^2 v = -c \frac{v}{L^2}$

where L may be thought of as being a characteristic length, for example, the pore size d of the medium. Assuming

$$u = -\frac{\partial \phi}{\partial x} \qquad v = -\frac{\partial \phi}{\partial y}$$

the Navier-Stokes equations become

$$-\frac{\partial}{\partial x}(\frac{\partial \phi}{\partial t}) + \frac{\partial}{\partial x}\left[\frac{1}{2}(\frac{\partial \phi}{\partial x})^2 + \frac{1}{2}(\frac{\partial \phi}{\partial y})^2\right] = -\frac{1}{\rho}\frac{\partial p}{\partial x} + \frac{\mu c}{\rho d^2}\frac{\partial \phi}{\partial x}$$

$$-\frac{\partial}{\partial y}(\frac{\partial \phi}{\partial t}) + \frac{\partial}{\partial y}[\frac{1}{2}(\frac{\partial \phi}{\partial x})^2 + \frac{1}{2}(\frac{\partial \phi}{\partial y})^2] = -\frac{1}{\rho}\frac{\partial p}{\partial y} + \frac{uc}{\rho_d^2}\frac{\partial \phi}{\partial y} - g.$$

If μ , ρ are constant, and if

$$\frac{c}{d^2} = \frac{1}{K}$$

integration of the equations leads to

$$-\frac{\partial \phi}{\partial t} + \frac{1}{2} \left[\left(\frac{\partial \phi}{\partial x} \right)^2 + \left(\frac{\partial \phi}{\partial y} \right)^2 \right] + \frac{p}{\rho} - \frac{\chi \phi}{\beta K} + gy = f(t). \tag{5}$$

This equation reduces to the Darcy law in the case of steady flow provided the inertia terms in the square brackets, here representing the kinetic energy of the fluid per unit mass, can be neglected. Equation (5) with $\frac{\partial \Phi}{\partial t}$ set equal to zero and f(t) constant for steady flow then reduces to

$$\Phi = \frac{K}{\mathcal{U}}(p + \gamma \gamma) + constant$$

which is equivalent to Equation (2), if we identify k with $\frac{K}{\mathcal{K}}$. Although the above derivation omits some arguments usually presented in a rigorous approach, it is sufficient for present purposes. For the detailed discussion of these equations, see the book by Muskat (1946). For the problem under consideration here and outlined previously, the governing equations and boundary condition are summarized as follows:

The two-dimensional Darcy's equation in an isotropic medium is

$$\vec{q} = -\frac{K}{\mu} (\nabla p - \rho g \hat{j}). \tag{6}$$

The continuity equation in general form for a porous medium is

$$\nabla \cdot \stackrel{\frown}{\rho} \stackrel{=}{q} = - \theta \frac{\partial \rho}{\partial t} \cdot \bullet \tag{7}$$

^{*}See, for example, Collins (1961).

For incompressible fluids, ρ = constant. Then Equation (7) becomes

$$\nabla \stackrel{\longrightarrow}{\mathbf{q}} = 0. \tag{8}$$

The boundary conditions relevant to the problem are described in the following:

At solid boundaries normal velocities will vanish, which implies that the normal derivative of Φ must vanish there. Therefore, since Φ = kh, we have

$$v_n = 0$$
 and $\frac{\partial h}{\partial n} = 0$ (B1)

where n indicates the direction normal to the solid boundaries.

If there is a sharp interface between region 1 and region 2, the pressure on both sides of the interface will be the same. Therefore, the following expression for the elevation Y of a point on the interface may be derived by equating the two expressions for p_1 and p_2 obtained by solving $h = \frac{p}{r} + Y$ for p.

$$Y = \frac{\gamma_1}{\gamma_2 - \gamma_1} \left[\frac{\gamma_2}{\gamma_1} h_2 - h_1 \right]$$

or

$$Y = \frac{1}{\Gamma} \left[\frac{\chi_2}{\chi_1} h_2 - h_1 \right]$$
 (B2)

where
$$\Gamma = \frac{\gamma_2 - \gamma_1}{\gamma_1}$$
.

If the liquid 2 is under hydrostatic condition, the total head h_2 will be constant in region 2. In this case, if we take region 2 for the reference state, we may set $h_2 = 0$, and Equation (B2) becomes

$$Y = -\frac{1}{\Gamma} h_1.$$
 (B3)

Also, normal velocities are the same on both sides of the interface, and we have

$$(v_1)_n = (v_2)_n. \tag{B4}$$

C. Review of Literature

In the study of flow through porous media, the location and the movement of the interface between two fluids are of particular interest to hydrologists and petroleum engineers. Badon-Ghyben (1888) and Herzberg (1901) stated the hydrostatic equilibrium condition for a fresh water lens floating on top of salt water in a porous aguifer. Since then several researchers have investigated the more relevant case that either one of the two fluids or both are in motion. The most common assumption among researchers in this field is that the salt water is static. Todd (1953) and Kitagawa (1939) combined this assumption with the one-dimensional form of Darcy's law to determine the position of the interface as a function of steady fresh-water discharge. This is similar to the case of gravity seepage, the problem in which the Dupuit (1863)-Forchheimer (1886) theory is utilized. Hubbert (1940)

established a general description of the flow of two fluids at either side of a steady interface between fluids. For the case when only one fluid is in motion, the hodograph method has been applied to several particular cases. A "hodograph" is a representation of a dynamical system in which the co-ordinates are the velocity components of the particles of the system. Noteworthy of investigators reporting on this method are Henry (1959), Glover (1959), and Kidder (1956).

Several major contributions in the analysis of unsteady flow with emphasis on the movement of interface are those of DeWiest (1959), DeJosselin DeJong (1960), Kidder (1956), and Bear and Dagan (1964). DeWiest, in his work, discusses the gravity flow with a free surface. idea of considering the unsteady flow as a perturbation in time of the final steady state is used. The perturbation velocity potential satisfies Laplace's equation in a dimensionless hodograph plane. The boundary-value problem is then set up mathematically and a numerical example worked out. DeJosselin DeJong based his work on the concept of replacing the two different fluids by one hypothetical fluid and of treating the different fluid properties by use of singularities along the interface. By knowing the position of the interface and the boundary conditions at a certain moment, the subsequent motion of the interface can be computed. He gives a mathematical example for a two-fluid system contained in a confined

infinite aquifer of uniform thickness with interface initially at a vertical position. Kidder treats the case in which the interface motion is caused by gravitational force acting on the two liquids. A general solution is obtained by direct potential theory methods and employs a method of approximation similar to that used in the linear theory of water waves. The method is applicable only when the initial slope and curvature of the interface are not too large. In a very recent publication, Bear and Dagan derive approximate expressions for the movement of the interface in a confined coastal aquifer caused by a sudden change in the rate of seaward flow of fresh water. The solutions are based on the Dupuit assumption. The range of validity of each solution is determined by comparing it with results of experiments.

In the present work, the solution to the problem of determining the movement of the interface in the transient state is obtained by successively making use of the one-dimensional flow assumptions and the two-dimensional flow assumptions. In one-dimensional flow, the governing differential equations are replaced by finite-difference equations, and these are solved numerically. In two-dimensional flow, the interface is considered as a distribution of sources along it, and the concept of Green's function is utilized in solving the problem. A case of finite aquifer of rectangular shape with interface initially of the parabolic shape is solved. The two liquids are assumed incompressible and immiscible.

CHAPTER II

ONE-DIMENSIONAL ANALYSIS

A. Derivation of the Equations

For the first approximation one-dimensional flow is assumed, since the vertical component of the velocity is negligible in the major portion of the flow field.

The simplifications which are made in this part of the analysis are: incompressible flow, sharp interface, the specific geometry shown in Figure 4, and an isotropic porous medium. The profile of the porous medium is of rectangular shape with length b and depth d. For the example worked out $\frac{b}{d} = 20$ so that the interface in Figure 4 is much more nearly horizontal than it appears to be in the figure, and the one-dimensional flow assumption therefore seems reasonable. For this discussion y is measured positively downward as shown in Figure 4. Hence, in the equations of Chapter I, y must be replaced by d-Y. The two fluids are of specific weights Y_1 and Y_2 .

The initial interface position $Y_0(\mathbf{x})$ is assumed to be that corresponding to equilibrium conditions with the fluid in reservoir 1 at a level of \mathbf{a}_0 above the top of the rectangular region, while the level in reservoir 2

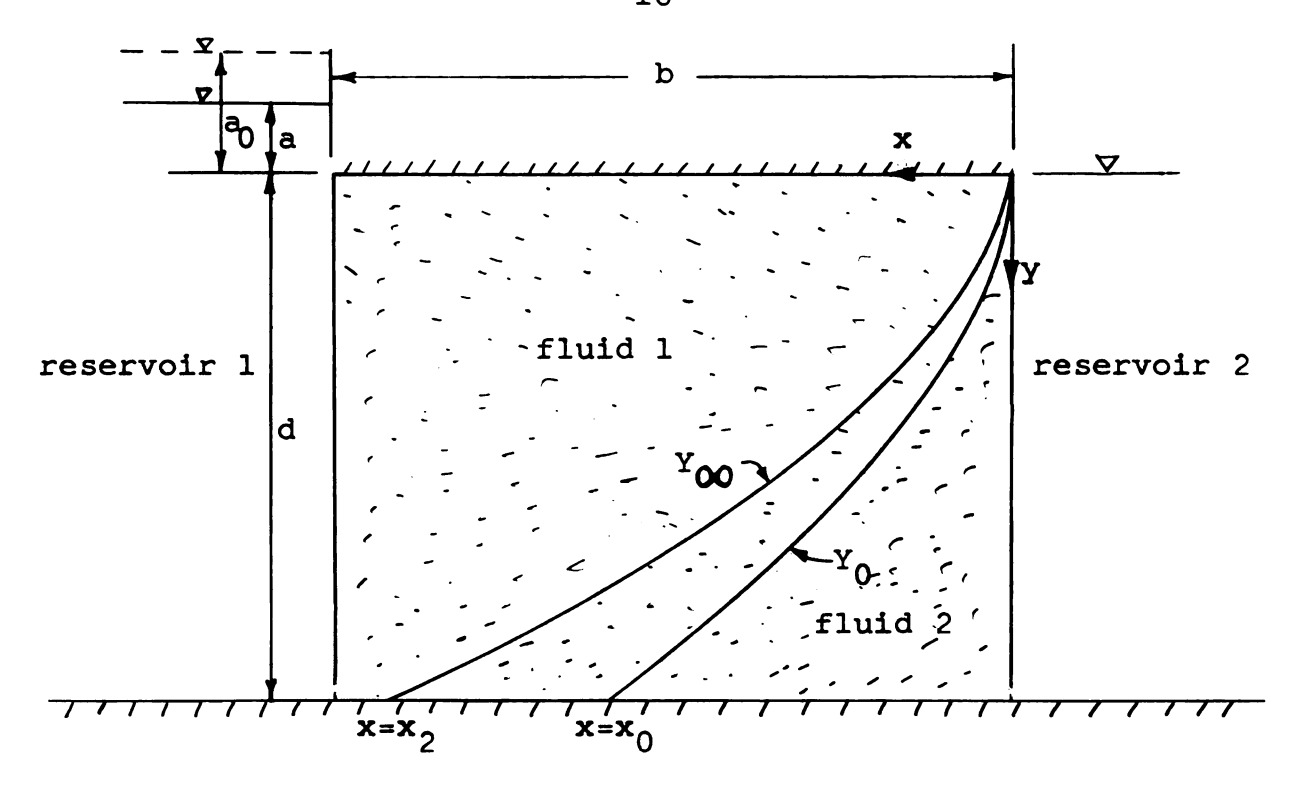


Figure 4.--Flow Geometry for One-dimensional Analysis

is zero. Then at t=0, the level of reservoir 1 is suddenly lowered to the new level "a," which then is maintained while the interface moves toward region 1 (upward and to the left in Figure 4) approaching the new equilibrium position $Y_{\infty}(x)$. The problem is to investigate the transient motion of the interface. Because the one-dimensional analysis appeared to be inadequate, only the early part of the transient motion was worked out in the numerical example to be presented below.

The applicable equations are Equation (1), which may be written as

$$\overrightarrow{q} = -k \nabla h, \qquad (9)$$

and Equation (8), which is repeated here

$$\nabla \cdot \overrightarrow{q} = 0. \tag{8}$$

The one-dimensional flow analysis supposes that in either of the two regions the flow velocity is horizontal and independent of y. If Q_1 is the total volume flow rate through a cross section $\mathbf{x} = \text{constant}$ of region 1, considered positive for flow to the right, and \mathbf{u}_1 is the horizontal velocity component there, positive for flow to the left, then $Q_1 = -\mathbf{u}_1 \mathbf{Y}$ since \mathbf{Y} is the distance down to the interface, or $Q_1 = -\mathbf{u}_1 \mathbf{d}$ at a section to the left of the point where the interface intersects the bottom of rectangle in Figure 4. Similarly the flow rate and velocity in region 2 below the interface are related by

$$Q_2 = -(d - Y)u_2$$

Applying the assumptions indicated above and shown by Figure 4, Equation (9) becomes

$$u_1 = -k_1 \frac{dh_1}{dx}$$

in the zone 1, and we have

$$Q_1 = k_1 Y \frac{dh_1}{dx}. \tag{10}$$

If zone 2 is assumed to be static, the boundary condition (B3) of Chapter I, part B applies, whence

$$\frac{dh_1}{dx} = \frac{\gamma_2 - \gamma_1}{\gamma_1} \frac{dy}{dx} = \Gamma \frac{dy}{dx} . \tag{11}$$

(The sign change is necessary because Y is now positive downward.) When this is substituted into Equation (10), that equation can be integrated to yield

$$y^2 = \frac{2Q_1}{\Gamma^{k_1}} x \tag{12}$$

if we impose the condition that Y = 0 at x = 0. This is the equation of the steady interface for any specified value of Q_1 .

Substituting Equation (B3), with a sign change, into Equation (10) and integrating with respect to \mathbf{x} , we have

$$Q_1 = \frac{1}{2} \frac{k_1}{\Gamma} \frac{h_1^2}{x} \qquad \text{for} \quad 0 \le x \le x_0$$

where we have used the condition $h_1 = 0$ at x = 0. For $x > x_0$, integration of Equation (10) for Y = d = constant with x = b when $h_1 = a$, gives

$$Q_1(x - b) = k_1 d(h - a)$$

or

$$Q_1 = \frac{k_1 d(h_1 - a)}{x - b} \quad \text{for} \quad x_0 \le x \le b.$$

If these two expressions for Q_1 are equated with $\mathbf{x} = \mathbf{x}_1$, noting from (B3) that $h_1 = \prod d$, the following relation between the level "a" in reservoir 1 and the co-ordinate \mathbf{x}_1 , where the transient interface intersects the bottom of the aquifer, is established

$$\frac{a}{d} = \frac{\Gamma}{2}(1 + \frac{b}{x_1}). \tag{13}$$

The resulting Q_1 for this relation is, after solving for $\frac{b}{x_1}$ and substituting into one of the equations for Q_1

$$Q_{1} = \frac{1}{2}k_{1}d(\frac{d}{b}) \Gamma \frac{b}{x_{1}}$$

$$= k_{1}(\frac{a}{d})d - \frac{1}{2}k_{1}(\frac{d^{2}}{b}) \qquad (14)$$

Darcy's equations are:

$$Q_1 = k_1 Y \frac{\partial^h_1}{\partial x} \tag{15}$$

$$Q_2 = k_2(d - Y) \frac{\partial^h 2}{\partial x}$$
 (16)

The continuity equation for region 1 is, after integrating two-dimensional form of Equation (8) from the upper boundary to the interface,

$$\int_{0}^{Y} \left(\frac{\partial u_{1}}{\partial x} + \frac{\partial v_{1}}{\partial y} \right) dy = -\theta \frac{\partial}{\partial t} \int_{0}^{Y} dy$$

= temporal rate of decrease
 of fluid caused by interface movement

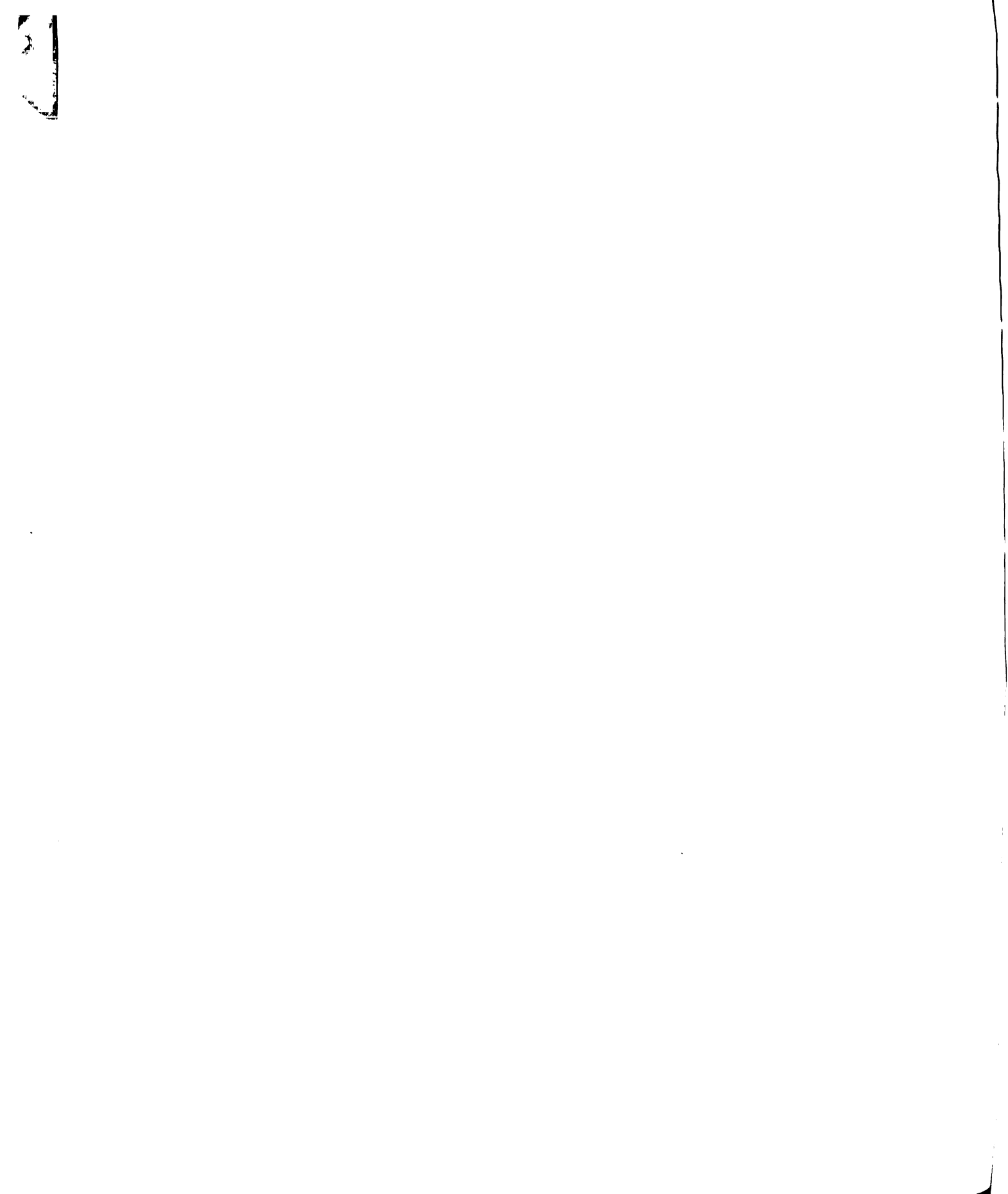
which then reduces to

$$\left(\frac{\partial^{\mathbf{u}}_{1}}{\partial \mathbf{x}} \mathbf{Y}\right) + \mathbf{u}_{1} \frac{\partial \mathbf{Y}}{\partial \mathbf{x}} + \theta \frac{\partial \mathbf{Y}}{\partial \mathbf{t}} = 0 \tag{17}$$

where the bar indicates a mean value.

For one-dimensional flow, $\frac{\partial^{u_1}}{\partial x}$ = constant across the cross section and since $Q_1 = Yu_1$

^{*}See p. 35 of "Advanced Mechanics of Fluids" by Hunter Rouse (editor).



$$Y \frac{\partial^{u_1}}{\partial x} = \frac{\partial^{Q_1}}{\partial x} - u_1 \frac{\partial Y}{\partial x}.$$

Therefore, Equation (17) becomes

$$\frac{\partial^{Q} 1}{\partial x} = -\theta \frac{\partial Y}{\partial t}. \tag{18}$$

Similarly, for region 2

$$\frac{\partial Q_2}{\partial \mathbf{x}} = + \theta \frac{\partial Y}{\partial t} . \tag{19}$$

Adding (18) and (19) and integrating with respect to ${\bf x}$ yields

$$Q_1 + Q_2 = f(t)$$
.

Alternatively, a definite integration with respect to x from 0 to b yields, after substituting (14) through (16)

$$\int_{0}^{\mathbf{x}_{1}} [k_{1} Y \frac{\partial^{h_{1}}}{\partial \mathbf{x}} + k_{2} (d-Y) \frac{\partial^{h_{2}}}{\partial \mathbf{x}}] d\mathbf{x} + \int_{\mathbf{x}_{1}}^{b} k_{1} d\frac{\partial^{h_{1}}}{\partial \mathbf{x}} d\mathbf{x}$$

$$Q_{T} = Q_{1} + Q_{2} = \frac{1}{2}k_{1}\frac{d^{2}}{b}\Gamma[\frac{2a}{\Gamma d} - 1] = constant.$$
 (20)

Equation (20) indicates that Q_T remains constant during the transient state. The expression in Equation (20) is equivalent to that in (14) as can be seen by solving (13) for $\frac{\mathbf{x}_1}{\mathbf{b}}$ and substituting in (14). This is to be expected, since at $\mathbf{x}_1 \le \mathbf{x} \le \mathbf{b}$ the entire discharge is in zone 1.

B. Numerical Example

As a specific example, we will consider the porous medium in Figure 4 with the following properties:

$$\frac{b}{d} = 20, \quad \frac{x_1}{b} = 0.5, \quad \frac{x_2}{b} = 0.95, \quad \Gamma = \frac{2 - 1}{1} = \frac{1}{40}.$$

We take $\mathcal{M}_1 = \mathcal{M}_2$; then, since $k_1 = \frac{K\gamma_1}{\mathcal{M}_1}$ and $k_2 = \frac{K\gamma_2}{\mathcal{M}_2}$, we have $k_2 = \frac{\gamma_2}{\gamma_1} k_1$. Initially, an equilibrium condition prevails and Equation (13) yields $\frac{a_0}{d} = 1.5T$ corresponding to $\mathbf{x}_1 = 0.5\mathbf{b}$. The elevation \mathbf{a}_0 is then suddenly lowered to $\frac{a}{d} = 1.026T$ corresponding to an equilibrium interface with $\mathbf{x}_2 = 0.95\mathbf{b}$. At the initial steady state the flow rate is $Q_0 = \frac{1}{20}k_1dT$ according to Equation (20), and during the transient state and at the final steady state $Q_T = \frac{1}{38}k_1dT$.

Introduction of the following dimensionless variables allows for considerable simplification:

$$\Omega_1 = \frac{Q_1}{Q_T}, \quad \Omega_2 = \frac{Q_2}{Q_T}, \quad \mathbf{y}' = \frac{\mathbf{y}}{\mathbf{d}}, \quad \mathbf{x}' = \frac{\mathbf{x}}{\mathbf{d}},$$

$$h_1' = \frac{k_1 h_1}{Q_T}, \quad h_2' = \frac{k_2 h_2}{Q_T}, \quad t' = \frac{Q_T t}{\theta d^2}.$$

Equations (15), (16), (18), (19), (20), and (B2) become:

$$\Omega_{1} = y' \frac{\partial h_{1}'}{\partial x'}$$
(21)

$$\Omega_2 = (1 - y') \frac{\partial h_2'}{\partial x'}$$
(22)

$$\frac{\partial \Omega_1}{\partial \mathbf{x}'} = \frac{\partial \mathbf{y}'}{\partial \mathbf{t}'} \tag{23}$$

$$\frac{\partial \Omega}{\partial \mathbf{x}'} = -\frac{\partial \mathbf{y}'}{\partial \mathbf{t}'} \tag{24}$$

$$\Omega_1 + \Omega_2 = 1 \tag{25}$$

$$Y' = \frac{Q_T}{dk_1} \Gamma (h_1' - h_2').$$
 (26)

The initial and final positions of the interface are computed from Equation (12), using the values of Q_0 and Q_T respectively, given above in the paragraph preceding Equation (21), as:

$$Y_0^{'2} = 0.1x'$$
 (27)

$$Y_{00}^{\prime 2} = 0.0526x^{\prime}. \tag{28}$$

Immediately after the reservoir surface of liquid 1 is changed, the value of Q_1 on the interval $b \ge x \ge 0.5b$ is the final $Q_1 = Q_T$ because $Q_2 = 0$ here and $Q_1 + Q_2 = Q_T = constant$. Hence $\Omega_1 = 1$ on this interval, and since y' = 1 on this interval, Equation (21) integrates to yield $(h_f')_0 = x' + constant$. Therefore, we have for the initial distribution of h_1' to the left of x = 0.5b immediately after the lowering of the liquid 1 level to its final value:

$$(h_1')_0 = x' + 19$$
 $0.5b \le x \le b.$ (29)

The distribution of h'_1 and h'_2 to the right of $\mathbf{x} = 0.5b$ is obtained by substituting (21) and (22) into (25) together with (27) yielding, after substituting the numerical data,

$$(h_1')_0 = \frac{2.69}{\sqrt{20}} \sqrt{x'} - 0.0455x' \qquad 0 \le x \le 0.5b \quad (30)$$

and

$$(h_2')_0 = -0.0455x'$$
 $0 \le x \le 0.5b$. (31)

Computed results of (29), (30), and (31) are plotted in Figure 5.

C. Finite-difference Solution Procedure

The difference equations corresponding to Equations (21) through (26) are:

$$(\Omega_1)_{i,j} = Y'_{i,j} \frac{(h'_1)_{i+1,j} - (h'_1)_{i-1,j}}{2(\Delta x')}$$
 (21A)

$$(\Omega_2)_{i,j} = (1 - y'_{i,j}) \frac{(h'_2)_{i+1,j} - (h'_2)_{i-1,j}}{2(\Delta x')}$$

$$\frac{(\Omega_{1})_{i+1,j} - (\Omega_{2})_{i-1,j}}{2(\Delta x')} = \frac{Y_{i,j+1} - Y_{i,j}}{\Delta t'}$$
(23A)

$$\frac{(\Omega_2)_{i-1,j} - (\Omega_2)_{i+1,j}}{2(\Delta x')} = \frac{y'_{i,j+1} - y'_{i,j}}{\Delta t'}$$
(24A)

$$(\Omega_1)_{i,j} + (\Omega_2)_{i,j} = 1$$
 (25A)

$$y_{i,j}' = \frac{Q_T}{k_1 d} \Gamma[(h_1')_{i,j} - (h_2')_{i,j}].$$
 (26A)

In these equations, the index i refers to the x' increments while j refers to the t' increments. The numerical computations are carried as follows:

- 1) Choose suitable intervals for $\Delta x'$ and $\Delta t'$.
- 2) From Equation (23A) compute, starting with j = 0

$$y'_{i,j+1} = \frac{(\Omega_1)_{i+1,j} - (\Omega_1)_{i-1,j}}{2(\frac{\Delta x'}{\Delta t'})} + y'_{i,j}.$$

3) Substitute Equations (21A) and (22A) into Equation (25A), replacing j by j + 1. Equation (26) is then substituted into the resulting equation to eliminate (h'1)i+1,j+1 and (h'1)i-1,j+1, yielding

$$\frac{(h_2')_{i+1,j+1} - (h_2')_{i-1,j+1}}{2(\Delta x')} = 1 - \frac{0.95}{\Delta x'} y_{i,j+1}'$$

$$(y'_{i+1,j+1} - y'_{i-1,j+1}).$$

4) The equation obtained in step (3) is then substituted into Equation (22A), giving

$$(\Omega_1)_{i,i+1} = (y'_{i,i+1})$$
 °

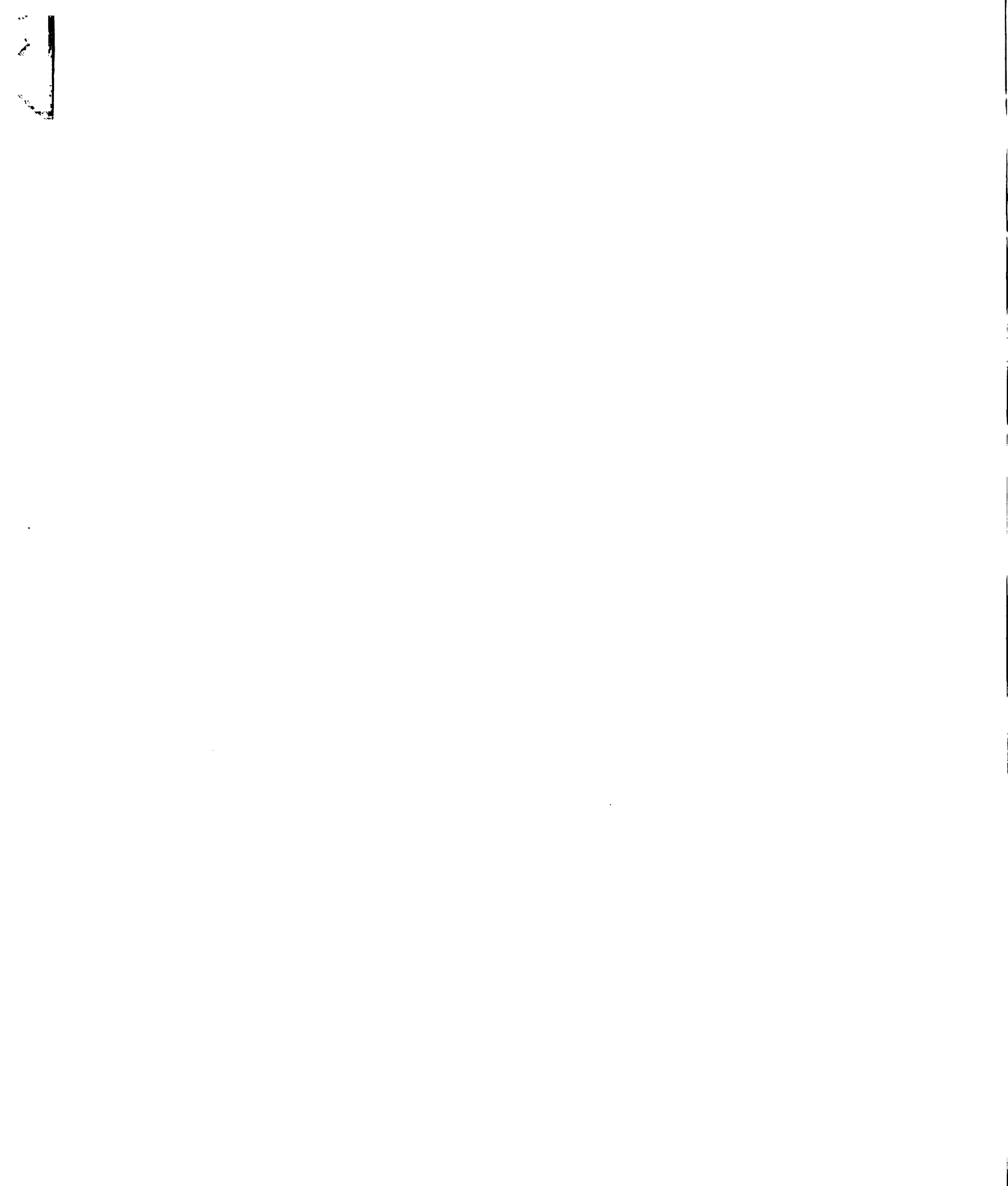
$$\left[1 + \frac{0.95}{\Delta x} (y_{i+1,j+1} - y_{i-1,j+1}) (1 - y_{i,j+1})\right].$$

- 5) $(\Omega_2)_{i,i+1}$ is then obtained from Equation (25A).
- 6) Repeat the steps(2) through (5) for new increments of j.

D. Results and Discussion

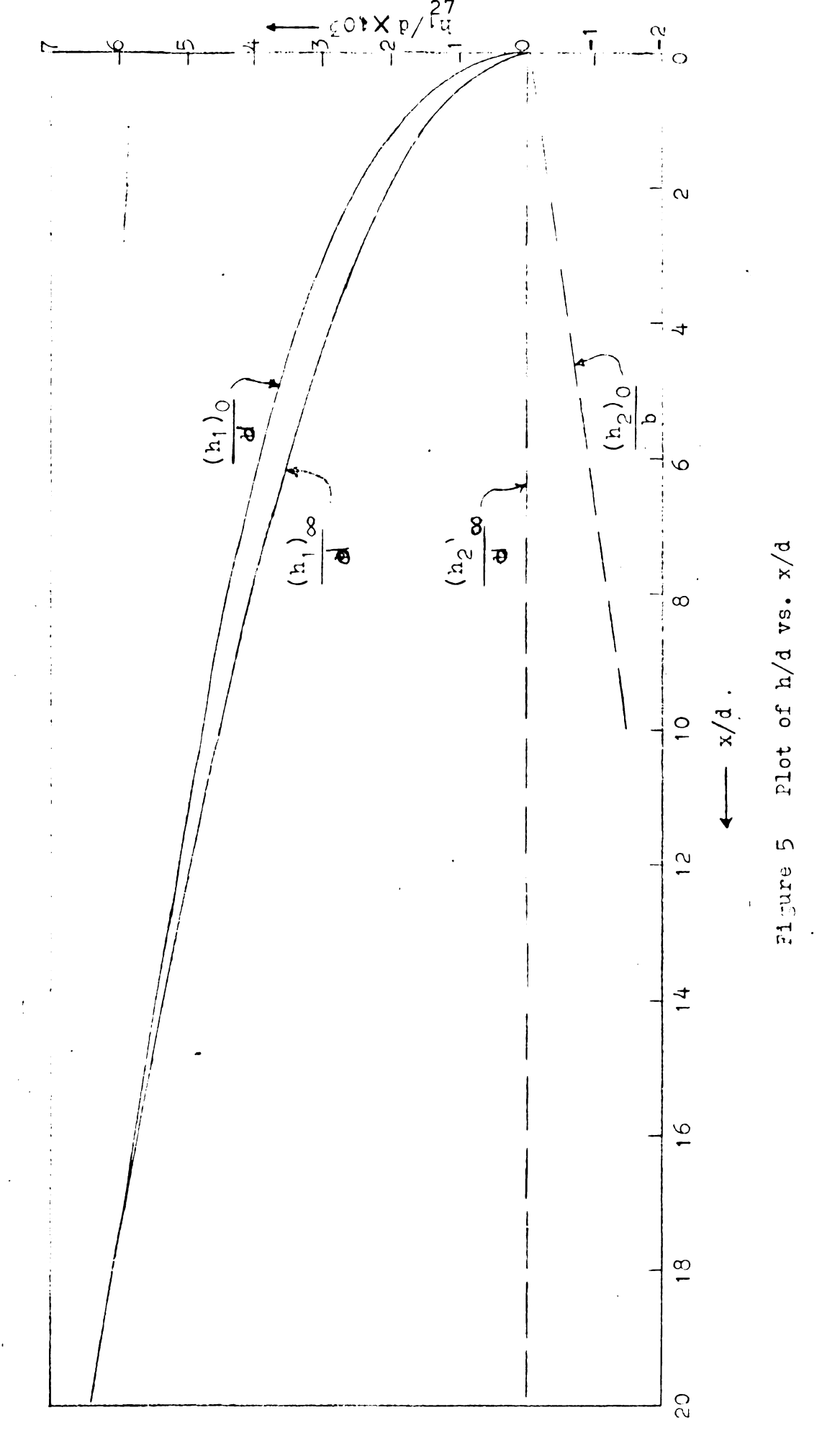
A numerical example with $\Delta x' = 1$ and $\Delta t' = 1$ was carried out, and the resulting interface locations corresponding to t' = 1 and t' = 2 are shown in Figure 6. This

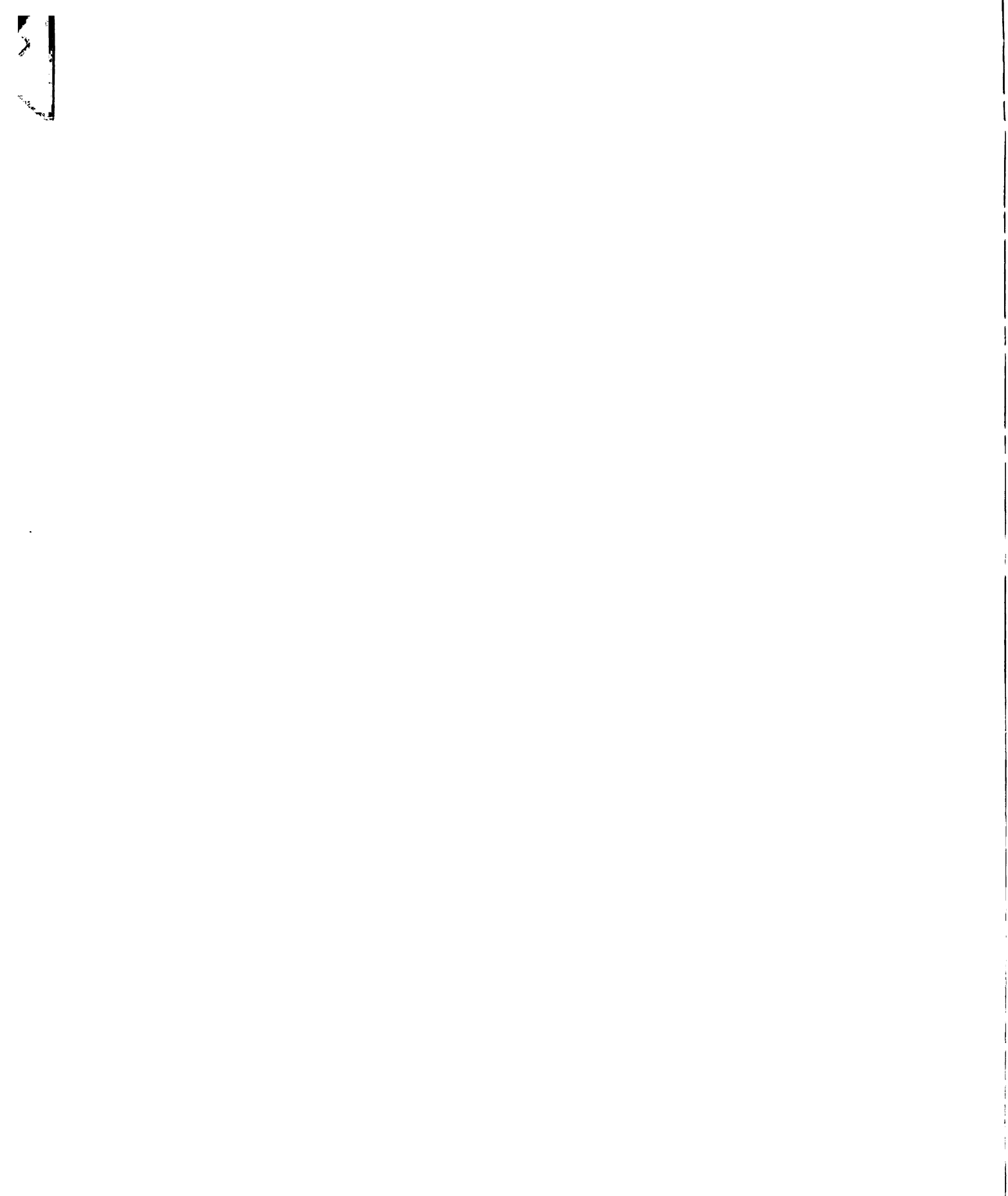
increment in x' is equivalent to dividing the entire length of the rectangle into twenty intervals. Since the initial interface occupied only half the length, it amounts to dividing the initial interface into ten equal horizontal intervals. The time interval was selected arbitrarily, to be checked for reasonableness by requiring that the calculated motion of the interface during the time interval be small compared to the distance from the initial equilibrium position $Y_0(x)$ to the final equilibrium position $Y_{\infty}(x)$. These computations are designated as Case 1. Observation of Figure 6 reveals that the computed values of Y tend to go above the final steady state near the right-hand end of the flow field. This is not likely to be the case, since oscillation is not anticipated. The difficulty may be attributed to the relatively steep slope of the interface in this region, where the vertical component of the velocity is not negligible and therefore the one-dimensional analysis is not a good approximation. An attempt to improve this discrepancy was made by taking smaller intervals ($\Delta x' = 0.02$, $\Delta t' = 0.02$) in the difference equations. The results of this as shown by Figure 7 disclose a similar tendency. Here, the locations of the interface computed for t = 0.02 and t = 0.04 are plotted. is designated as Case 2. Another calculation was made after interchanging the initial and final positions of the interface, i.e., making the final steady-state position of the interface in the previous case the initial position of



the interface in this case. The result of this for t'=1 and t'=2 as given by Figure 8 indicates that the values of Y tend to fall far below the final steady state near the right end. This is designated as Case 3. Again, we are unable to overcome the difficulty mentioned in the previous case. All the data pertaining to Figures 5 through 8 are listed in Tables 1, 2, and 3.

The results obtained in these analyses lead to the conclusion that the one-dimensional approximation cannot be valid near the outflow end, though it may possibly be a good approximation elsewhere. The two-dimensional analysis will be used in the next chapter to yield a refined solution.





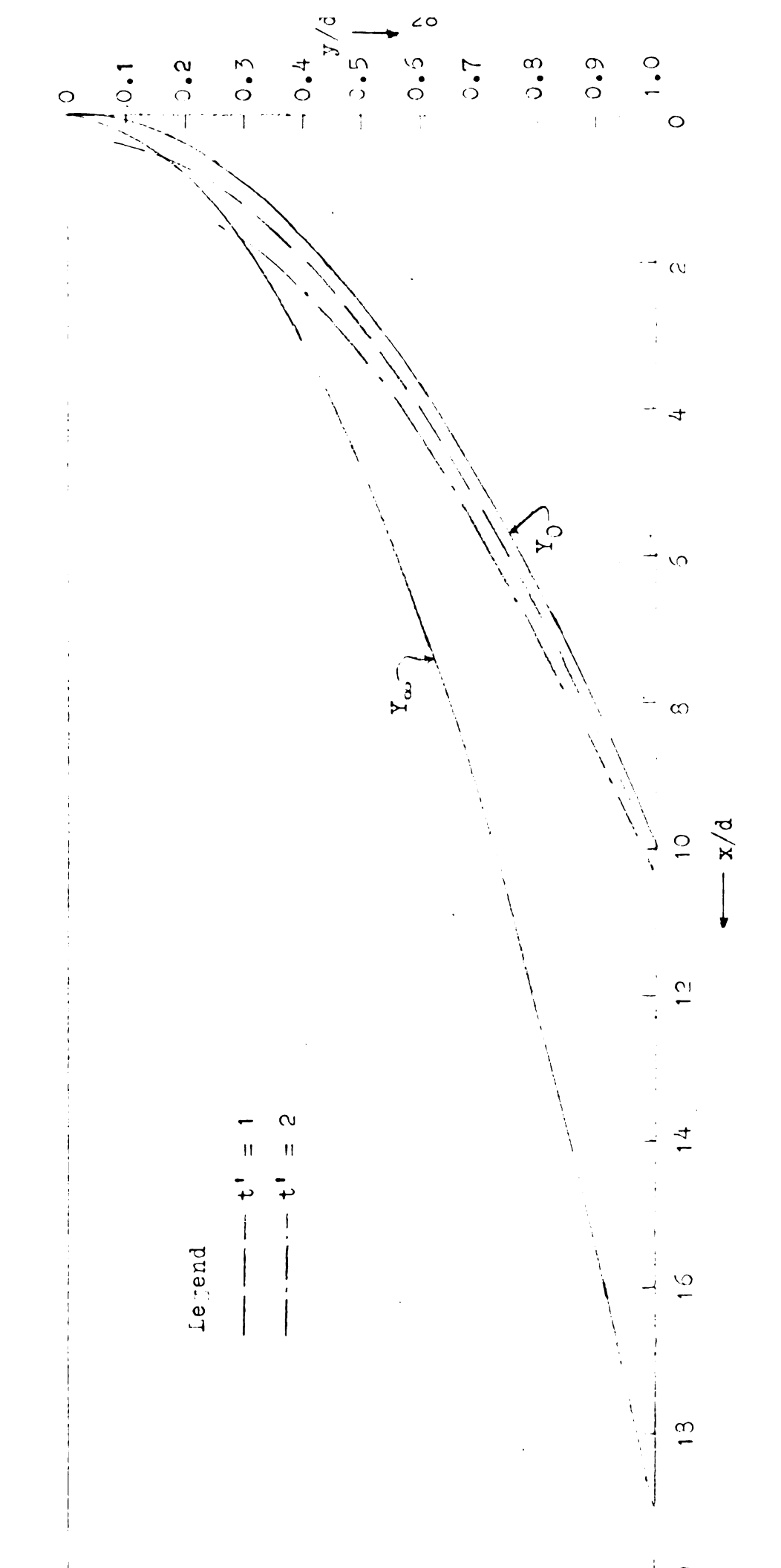


Figure 6 Movement of Interface--Jase 1

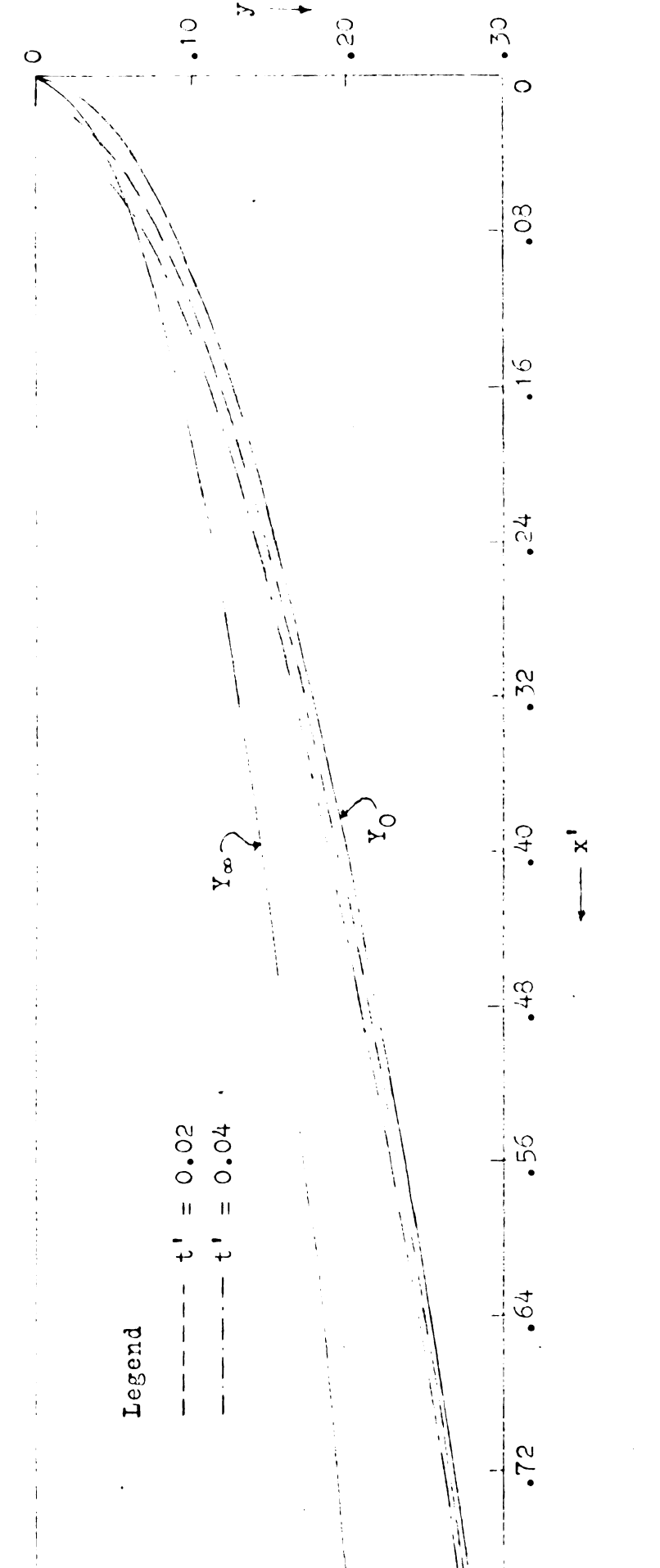
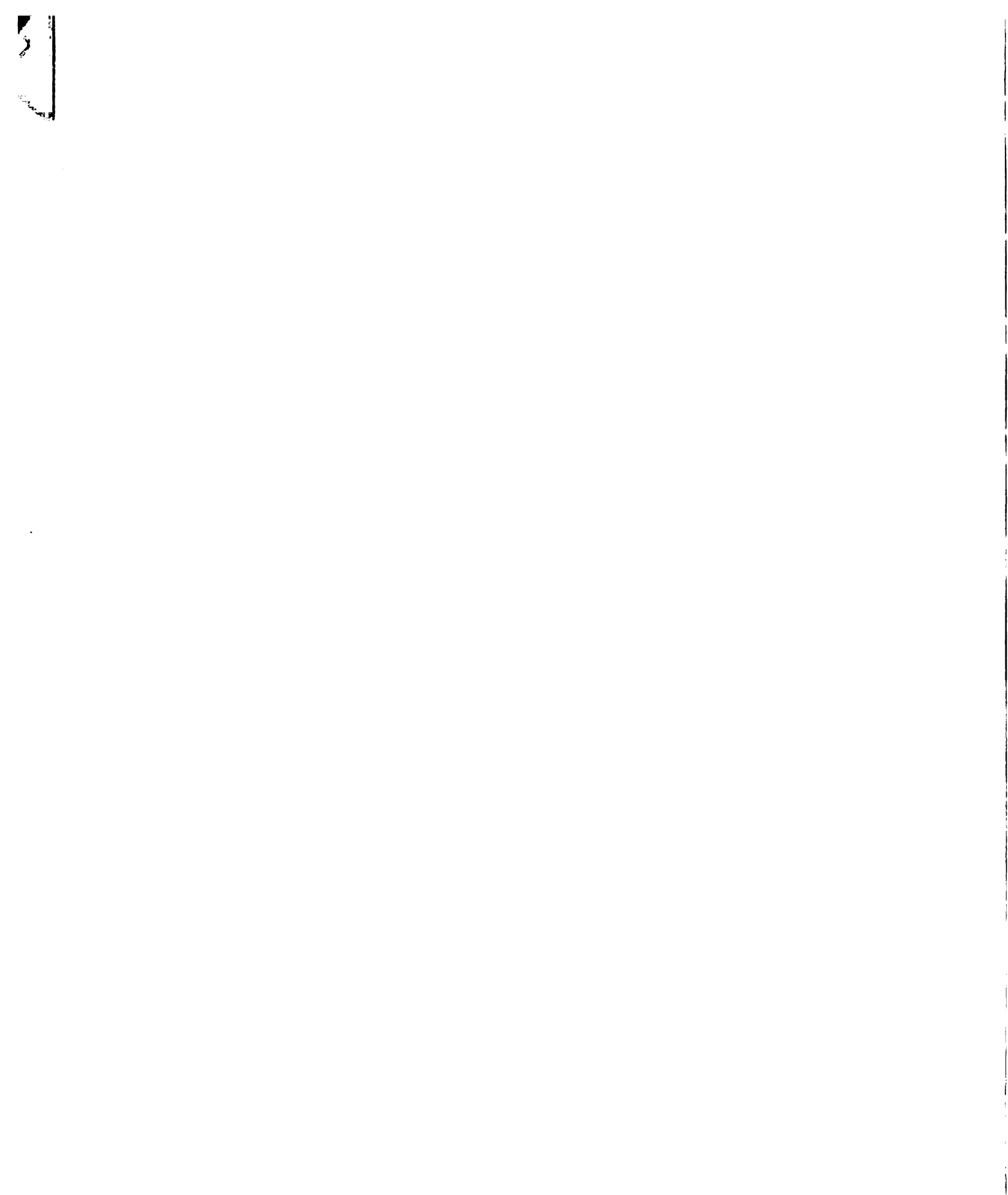


Figure 7 Movement of Interface--Case 2

000



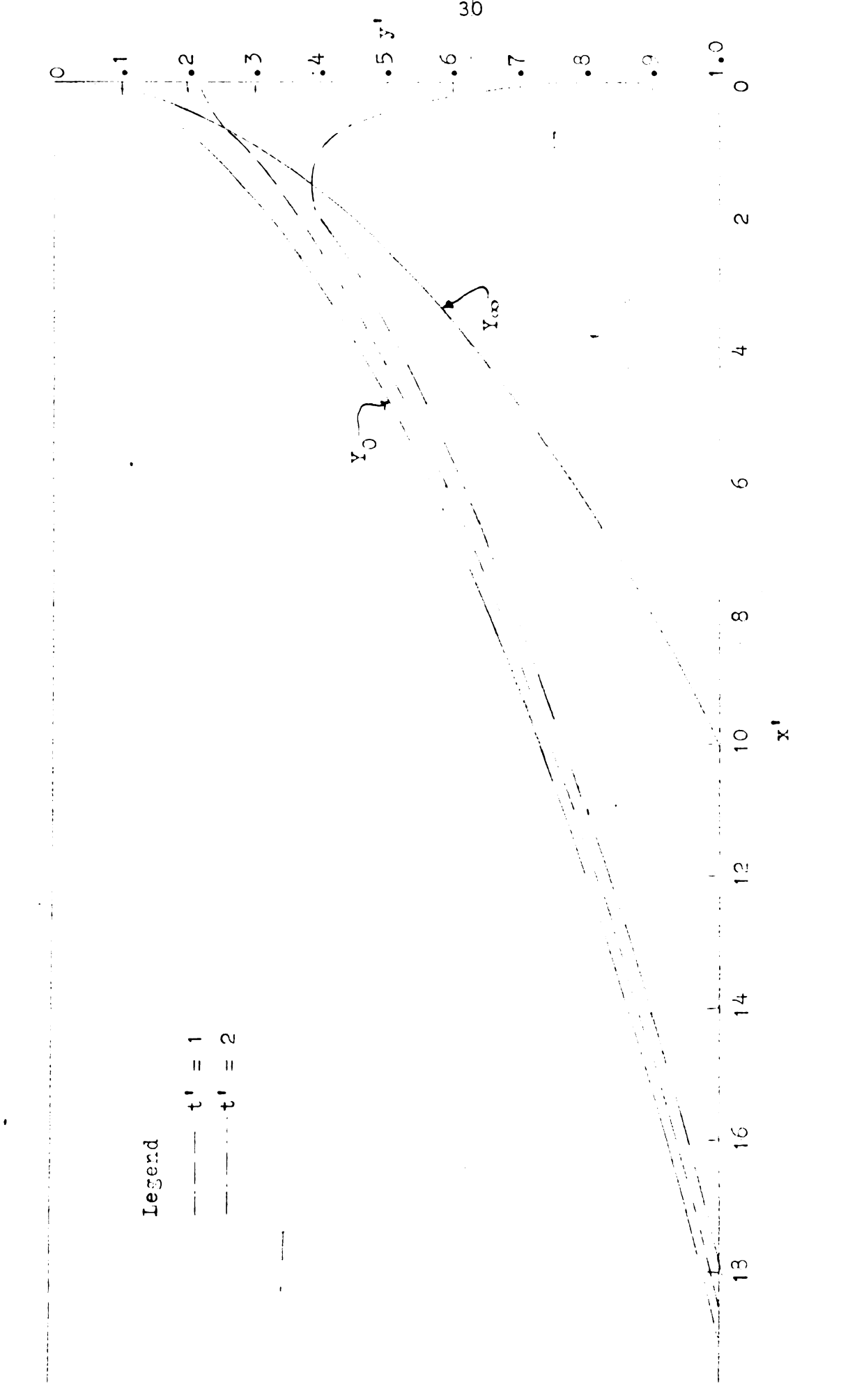


Figure 8 Movement of Interface--Case 3

	÷	TABLE 1 TABUL	TABULATION FOR FIGUR	FIGURES 5 AND 6		
>		$\frac{(h_1)_0}{d} \times 10^3$	$\frac{(h_2)_0}{d} \times 10^3$	$\frac{(h_1)_{00}}{d} \times 10^3$	Y ₁	
0		0	0	0	0	
2		•	-0.146	1.43	۲.	
.32		5	. 29	0	.34	
.39		9	.43	4.	.46	
.45		د ،	.58	ω	.56	
.51		9	.73	2,	.64	
.54		9	.87	4.	. 71	
.60		۲.	.02	ω	. 78	
0.648		സ	-1,170	4.05	0.844	
.68		9	,31	.	• 90	
.72		٠,	• 46	.5	.97	
• 76		6		.7		
, 79		1.		6		
.82		2		۲.		
.85		4°		സ		
.88		S		5		
.91				. 7		
.94		σ,		σ.		
.97		0		0		
900		2		2		
		4.		• 4		

Note Y_1 is the interface position for t=1 Y_2 is the interface position for t=2

TABLE 2 TABULATION FOR FIGURE 7

x /d	$^{\mathtt{Y}}\mathtt{1}$	Y ₂	x/ d	Y ₁	Y ₂
0	0				
0.02	0.0157		0.42	0.1999	0.1920
0.04	0.0482		0.44	0.2048	0.1970
0.06	0.0655	0.0562	0.46	0.2105	0.2010
0.08	0.0794	0.0700	0.48	0.2151	0.2060
0.10	0.0900	0.0825	0.50	0.2196	0.2110
0.12	0.1005	0.0930	0.52	0.2240	0.2160
0.14	0.1103	0.1028	0.54	0.2284	0.2215
0.16	0.1195	0.1120	0.56	0.2326	0.2255
0.18	0.1272	0.1180	0.58	0.2368	0.2300
0.20	0.1344	0.1260	0.60	0.2409	0.2345
0.22	0.1423	0.1330	0.62	0.2450	0.2385
0.24	0.1489	0.1400	0.64	0.2490	0.2430
0.26	0.1552	0.1475	0.66	0.2529	0.2470
0.28	0.1613	0.1545	0.68	0.2568	0.2510
0.30	0.1672	0.1610	0.70	0.2606	0.2550
0.32	0.1739	0.1680	0.72	0.2653	0.2590
0.34	0.1794	0.1730	0.74	0.2680	0.2630
0.36	0.1847	0.1775	0.76	0.2717	0.2670
0.38	0.1899	0.1830	0.78	0.2763	0.2715
0.40	0.1950	0.1875	0.80	0.2788	0.2760

Note Y_1 is the interface position for t = 0.02 Y_2 is the interface position for t = 0.04

TABLE 3 TABULATION FOR FIGURE 8

x/ d	YO	Y00	Y ₁	Y ₂
0	0	0		
1	0.229	0.316	0.306	
2	0.324	0.447	0.364	0.393
3	0.397	0.548	0.429	0.458
4	0.459	0.633	0.486	0.512
1 2 3 4 5	0.512	0.707	0.536	0.560
	0.562	0.775	0.584	0.606
6 7	0.607	0.837	0.627	0.647
8	0.648	0.895	0.667	0.686
8 9	0.688	0.949	0.706	0.724
10	0.725	1.000	0.742	0.759
11	0.760		0.776	0.792
12	0.794		0.810	0.825
13	0.827		0.842	0.85 7
14	0.858		0.872	0.887
15	0.888		0.902	0.916
16	0.917		0.931	0.944
17	0.945		0.958	0.971
18	0.973		0.986	
19	1.000			

Note Y_1 is the interface position for t = 1

 Y_2 is the interface position for t = 2

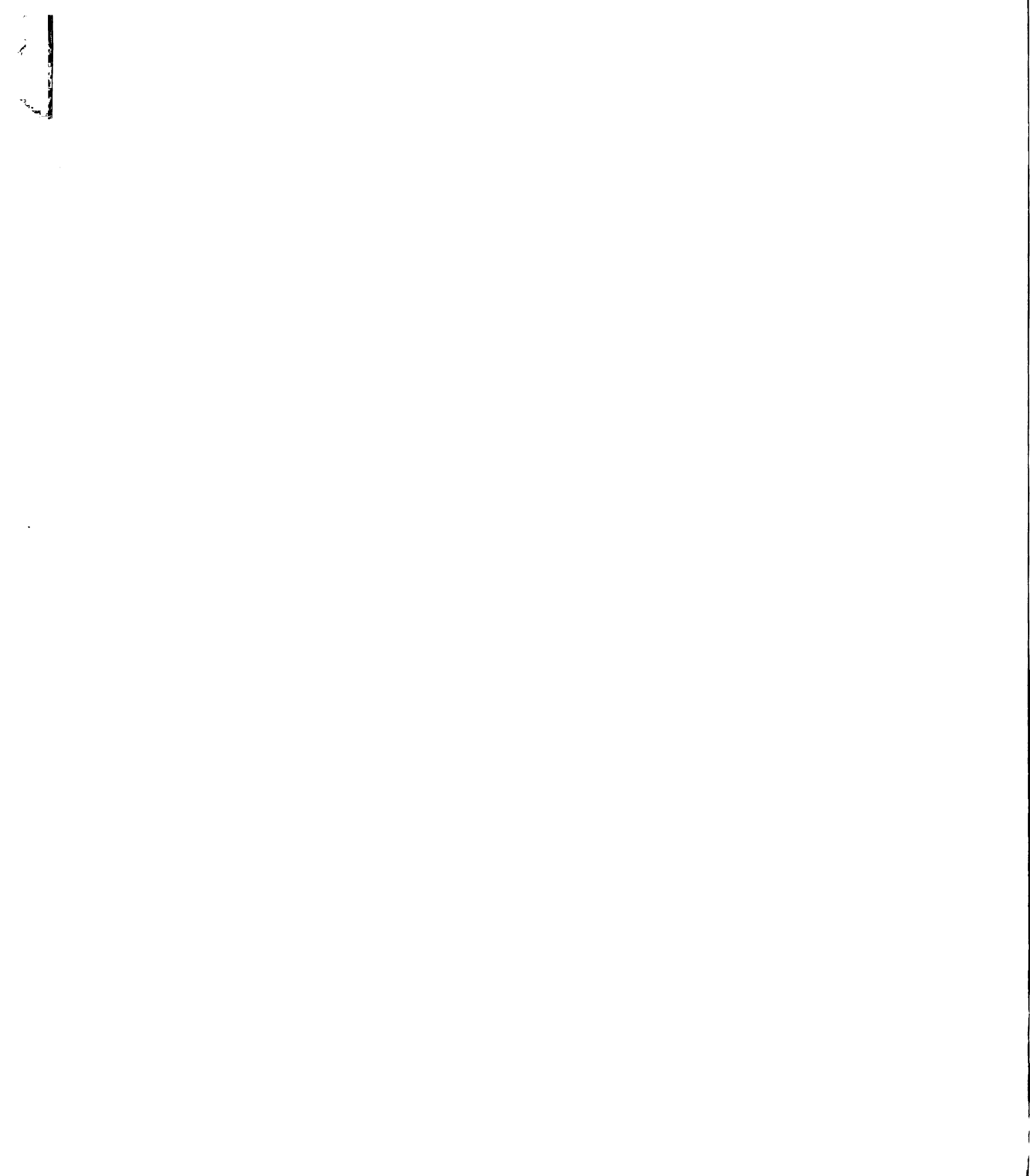
CHAPTER III

TWO-DIMENSIONAL ANALYSIS

A. Formulation of the Boundary-value Problem

The one-dimensional analysis as presented in the previous chapter gives a reasonable result in the major portion of the flow field. The inaccuracy near the outflow seepage face is caused by the fact that the vertical component of the velocity in this region is no longer negligible. It is, therefore, the purpose of this chapter to analyze the problem with the assumption that the flow is two-dimensional. To make the problem mathematically tractable, a porous medium of rectangular shape with length b and depth d, as shown in Figure 9 will once again be considered. In this chapter the y-co-ordinate is again measured positively up from the bottom, as it was in Chapter I, and the sign change required for y in Chapter II is not needed. The assumptions of incompressible flow and a sharp interface are also made. The specific geometry with the appropriate boundary conditions is shown in Figure 9. Note that the boundaries AF and CDE are impervious.

Region 1 is occupied by a fluid of density $\frac{y_1}{g}$ while region 2 is occupied by that of density $\frac{y_2}{g}$, where



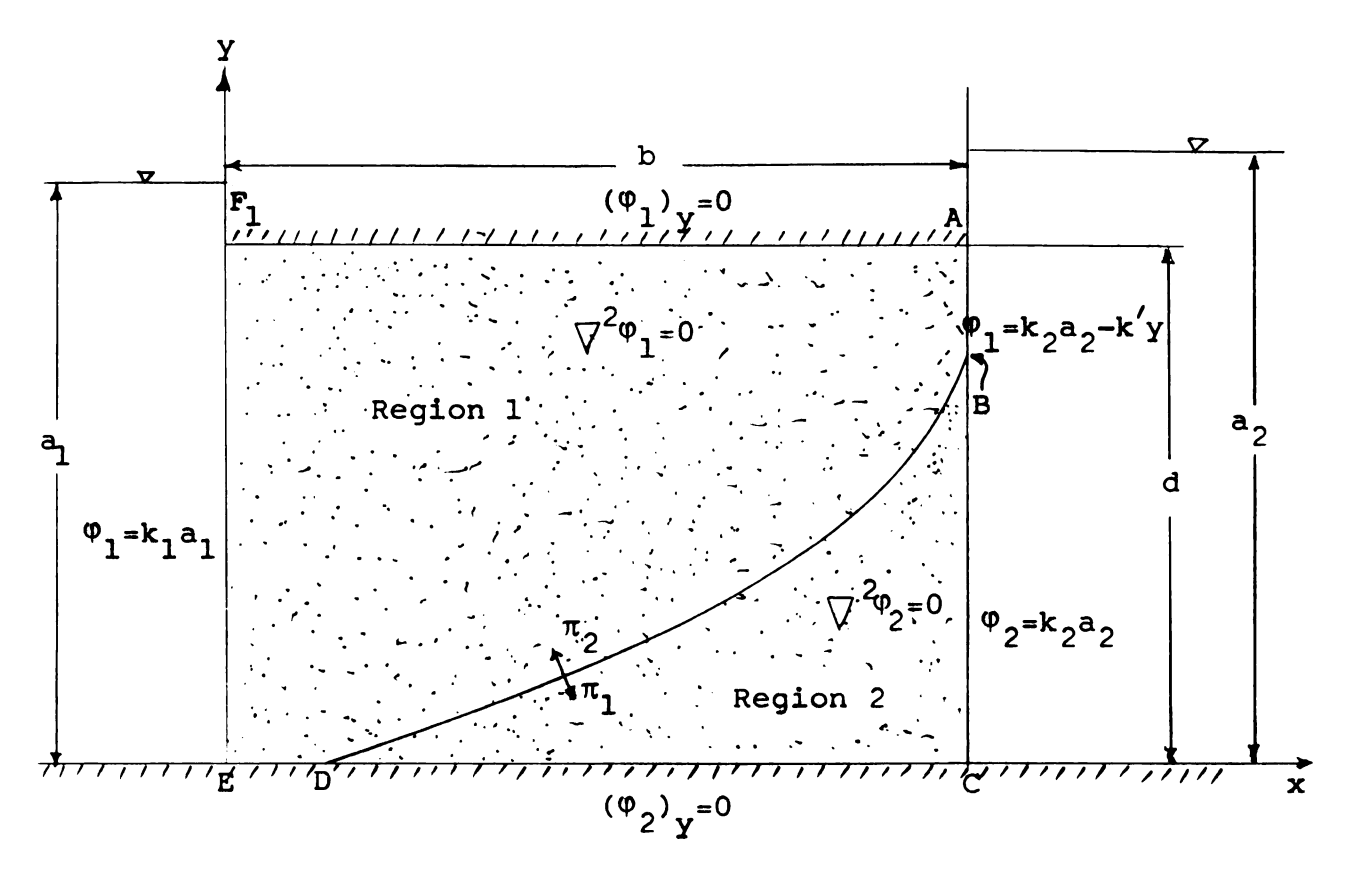
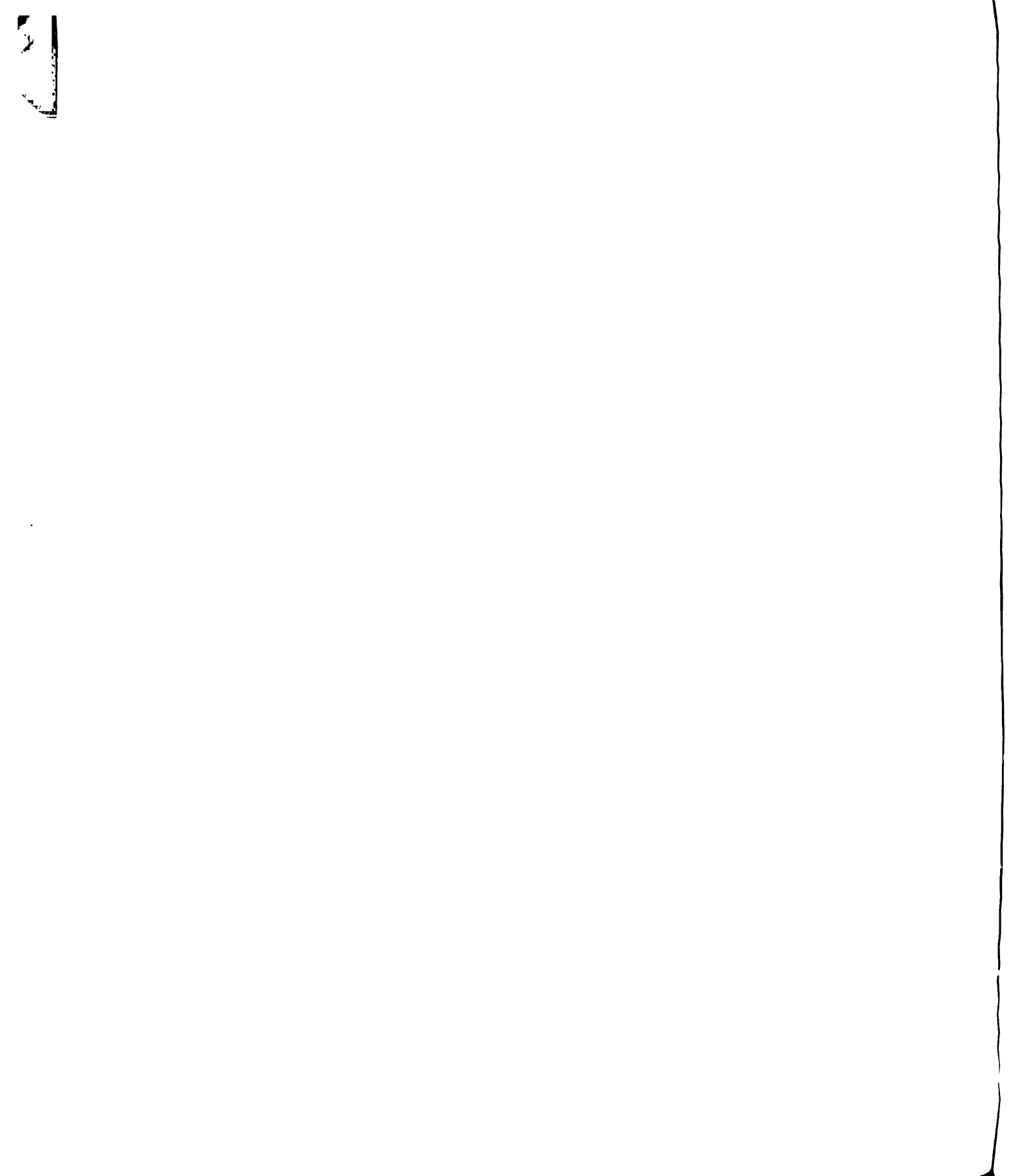


Figure 9. -- Geometry of Flow and Boundary Conditions

 $\gamma_2 > \gamma_1$. The method of solution applies at any time of the transient motion to calculate the next step of the motion when the two fluids are in a non-equilibrium state. In the example to be presented the initial interface position is a parabolic approximation to the known equilibrium configuration for a certain total discharge rate Q. Transient motion of the interface is then examined under the assumption that at t = 0 the discharge rate is changed to a higher value and maintained constant. Such a change in discharge rate could be produced physically by raising the level of the fluid in reservoir 1, and this would cause the interface to move to the right. The boundary



conditions indicated are obtained from the fact that the reservoirs are under static conditions and that the surfaces AF and CDE are impervious. Under static conditions the total head is independent of y since the pressure head increases with depth by an amount equal to the decrease in elevation. Thus on FE we have $\varphi_1 = k_1 a_1$ and on BC $\varphi_2 = k_2 a_2$. Since the normal derivative must be zero at the impervious top and bottom boundaries, we have $(\varphi_1)_y = 0$ on AF and ED and $(\varphi_2)_y = 0$ on DC, where the subscript denotes the partial derivative with respect to y. The boundary condition for φ_1 on AB is derived below as Equation (38).

Darcy's law for homogeneous two-dimensional flow through porous media is valid everywhere in the porous medium except along the interface. Therefore, we have

$$u_{1} = -k_{1} \frac{\partial^{h}_{1}}{\partial x}, \qquad v_{1} = -k_{1} \frac{\partial^{h}_{1}}{\partial y},$$

$$u_{2} = -k_{2} \frac{\partial^{h}_{2}}{\partial x}, \qquad v_{2} = -k_{2} \frac{\partial^{h}_{2}}{\partial y}$$
(32)

where the subscripts refer to the appropriate zones.

If we introduce the velocity potentials $\Phi_1 = k_1 h_1$ and $\Phi_2 = k_2 h_2$ into Equations (32) we have

$$u_{1} = -\frac{\partial \Phi_{1}}{\partial \mathbf{x}}, \qquad v_{1} = -\frac{\partial \Phi_{1}}{\partial \mathbf{y}},$$

$$u_{2} = -\frac{\partial \Phi_{2}}{\partial \mathbf{x}}, \qquad v_{2} = -\frac{\partial \Phi_{2}}{\partial \mathbf{y}}$$
(33)

or in vector form $\overrightarrow{q} = -\nabla \varphi$. (34)

Since the continuity equation must be satisfied, we have, from Equation (8) for incompressible flow, the Laplace's equation

$$\nabla^2 \Phi = 0. \tag{35}$$

Equation (35) applies in regions 1 and 2, respectively, but does not apply across the interface.

The boundary conditions along the seepage face AB and the interface BD are derived as follows. The pressure is continuous across these faces. Therefore, the condition

$$p = (\frac{\phi_1}{k_1} - y) \gamma_1 = (\frac{\phi_2}{k_2} - y) \gamma_2$$
 (36)

has to be imposed on them. For the vertical seepage face AB, where $\Phi_2 = k_2 a_2$, Equation (36) becomes

$$\phi_1 = k_1 \frac{\gamma_2}{\gamma_1} a_2 - \gamma (\frac{\gamma_2}{\gamma_1} - 1) k_1.$$
 (37)

To further simplify the analysis, let $\mu_2 = \mu_1^*$ Then, since

$$k_1 = \frac{K \gamma_1}{\mathcal{U}_1}$$
 and $k_2 = \frac{K \gamma_2}{\mathcal{U}_1}$

we have $\frac{\gamma_2}{\gamma_1}k_1 = k_2$; and, if we introduce $k' = (\frac{\gamma_2}{\gamma_1} - 1)k_1$,

Equation (37) reduces to

^{*}If the two liquids are fresh water and salt water, respectively, the viscosities are practically the same.

$$\varphi_1 = k_2 a_2 - k' y. \tag{38}$$

Similarly, for the interface BD

$$\phi_1 = \phi_2 - k_1 (\frac{\gamma_2}{\gamma_1} - 1) y = \phi_2 - k' y.$$
 (39)

Also, normal components of the velocities along the interface are the same on both sides and therefore

$$\frac{\partial^{\varphi_1}}{\partial^{n_1}} = -\frac{\partial^{\varphi_2}}{\partial^{n_2}} \tag{40}$$

since positive \mathbf{n}_1 and \mathbf{n}_2 are chosen outward from the respective regions and are therefore in opposite directions on the interface. We introduce the stream function ψ defined by

$$u = \frac{\partial \psi}{\partial x}, \qquad v = -\frac{\partial \psi}{\partial x}$$
 (41)

which with ϕ satisfies the Cauchy-Riemann equations

$$\frac{\partial \psi}{\partial \mathbf{y}} = -\frac{\partial \phi}{\partial \mathbf{x}}, \qquad \frac{\partial \psi}{\partial \mathbf{x}} = \frac{\partial \phi}{\partial \mathbf{y}}. \tag{42}$$

Differentiating Equation (39) with respect to s, the distance along the interface, yields

$$\frac{\partial \varphi_1}{\partial s} = \frac{\partial \varphi_2}{\partial s} - k' \frac{\partial y}{\partial s} \tag{43}$$

where s is defined positive from D toward B. In terms of ψ , Equation (43) becomes

$$-\frac{\partial \psi_1}{\partial n_2} = -\frac{\partial \psi_2}{\partial n_2} - k' \frac{\partial y}{\partial s}$$
 (44)

where we have used Equation (42) with local x and y axes

in the s and n_2 directions. Since $\frac{\partial \psi}{\partial n_2} = -\frac{\partial \psi}{\partial n_1}$, this becomes

$$\frac{\partial \psi_1}{\partial n_1} = \frac{\partial \psi_2}{\partial n_1} - k' \frac{\partial y}{\partial s}. \tag{45}$$

Also, Equation (40) becomes

$$\frac{\partial \psi_1}{\partial s} = \frac{\partial \psi_2}{\partial s} . \tag{46}$$

In summary, the problem, in terms of ψ , is to solve the governing equation $\nabla^2 \psi = 0$ with the boundary conditions shown in Figure 10. Subscripts x and n denote

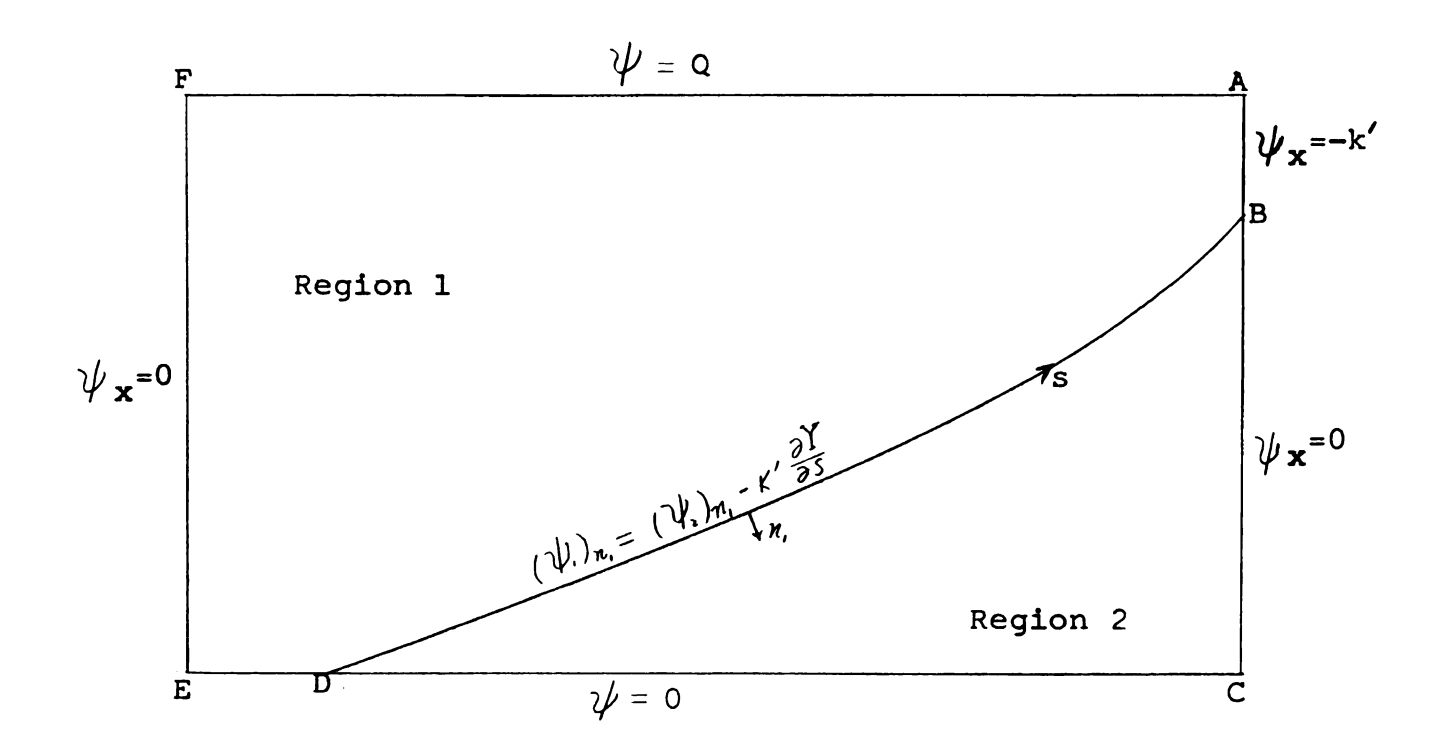


Figure 10.--Boundary Conditions in Terms of ψ partial derivatives. The boundary conditions on ψ along EF and AC are obtained from those on Φ shown in Figure 9, by using Equations (42). These equations also imply that

 ψ is constant along the top and bottom. If we arbitrarily set ψ = 0 along the bottom, then along the top ψ is equal to the total discharge Q, since along $\text{EF} \frac{\partial \psi}{\partial Y}$ is equal to u. The interface condition along DB was derived above as Equation (45). To simplify the problem one step further, a function ψ is introduced, defined by ψ = $\psi - \frac{Q}{d}y$. Then $\nabla^2 \psi = \nabla^2 \psi$ and the problem is to find a function ψ which satisfies Laplace's equation in region 1 and in region 2 with the boundary conditions shown in Figure 11.

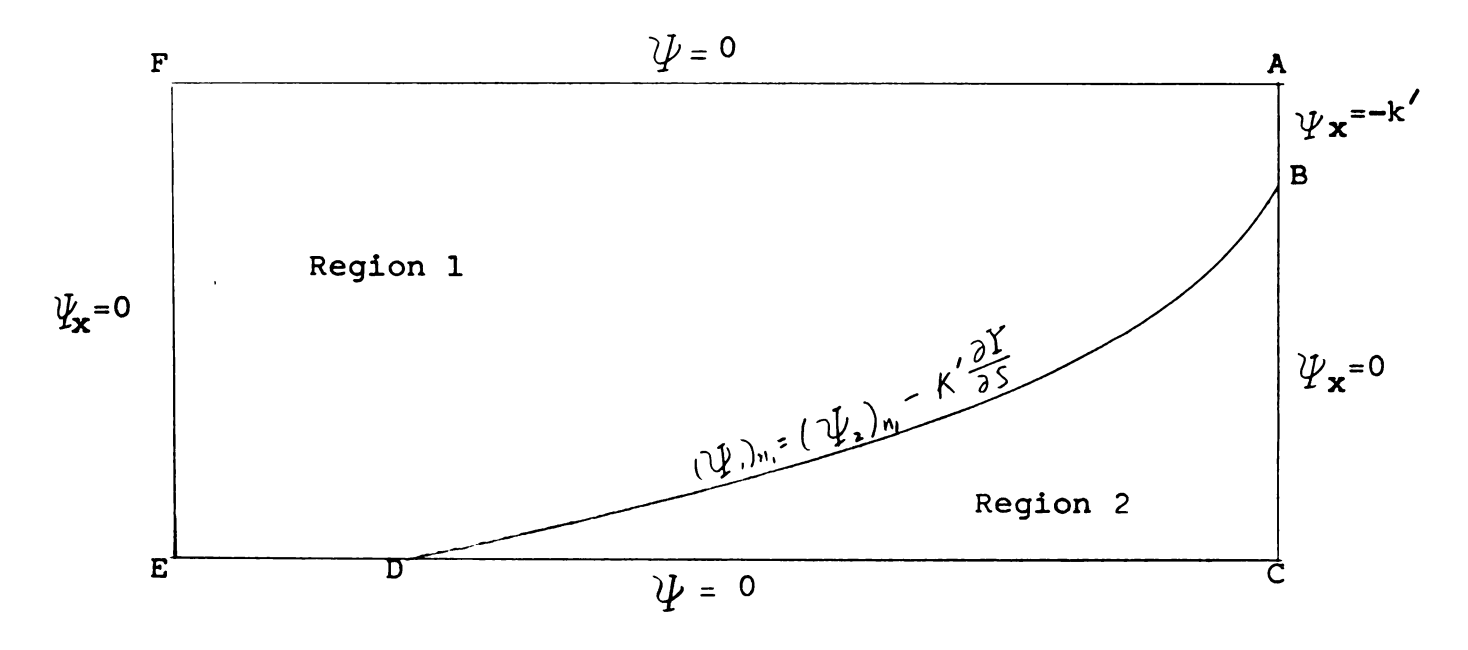


Figure 11.--Boundary Conditions in Terms of $\,\Psi\,$

B. Solution Procedure with Green's Function

Since a discontinuity exists along the interfaces DB and BA, the governing differential equation does not apply across them. The interface, with normal velocity discontinuity as shown in Figure 11, can be considered as

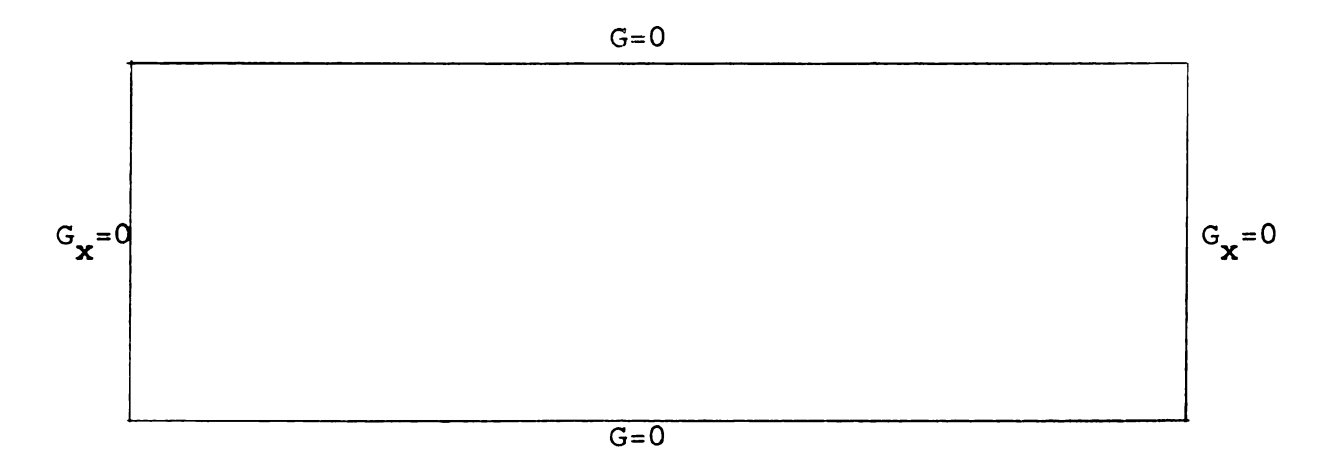


Figure 12. -- Boundary Conditions for G

a distribution of sources with sources intensity $f(\xi, \eta)$ per unit length, equal to the discontinuity in $\frac{\partial \psi}{\partial \eta}$. Here $\xi(s)$ and $\eta(s)$ are the rectangular co-ordinates of the source point specified by the arc-length parameter s. The details of solution for ψ are presented in Appendix V. The results are quoted below in Equations (47) to (49). The solution for $\psi(x,y)$ in either region is given in terms of a Green's function $G(x,y; \xi, \eta)$ as*

$$\Psi(\mathbf{x},\mathbf{y}) = -\int_{D}^{B} G(\mathbf{x},\mathbf{y}; \xi, \eta) \rho(\xi, \eta) ds +$$

$$\int_{B}^{A} G \frac{\partial \Psi}{\partial \mathbf{x}} d\mathbf{y} \tag{47}$$

where G is, for each value of f and f, a solution of Laplace's equation

^{*}See, for example, L. V. Kantorovich and V. I. Krylov, "Approximate Methods of Higher Analysis," pp. 71-72, and pp. 496-97 for Equations (47) and (48).

$$\frac{\partial^2 G}{\partial x^2} + \frac{\partial^2 G}{\partial y^2} = 0$$

in the whole rectangle, satisfying the boundary conditions shown in Figure 12.

The required function G is given by the double trigonometric series of Equation (48)

$$G(x,y; \xi, \eta) = -\frac{4}{\pi^2 \text{bd}} \sum_{m=1}^{\infty} \sum_{n=0}^{\infty} \alpha_n$$

$$\frac{\cos \frac{n\pi x}{b} \sin \frac{m\pi y}{d} \cos \frac{n\pi x}{b} \sin \frac{m\pi y}{d}}{\frac{n^2}{b^2} + \frac{m^2}{d^2}}$$
(48)

where

When we introduce the source strength $\rho = k' \frac{\partial y}{\partial s}$ on DB and $\rho = -k'$ on BA, Equation (47) takes the form

$$\Psi(\mathbf{x},\mathbf{y}) = -\int_{D}^{B} G[\mathbf{x},\mathbf{y}; \, f(\mathbf{s}), \, \eta(\mathbf{s})] \, \mathbf{k}' \frac{\partial \mathbf{y}}{\partial \mathbf{s}} \, d\mathbf{s} - \mathbf{k}' \int_{B}^{A} G(\mathbf{x},\mathbf{y}; \, \mathbf{b}, \, \eta) \, d\eta$$

$$= -\mathbf{k}' \int_{D}^{A} G[\mathbf{x},\mathbf{y}; \, f(\eta), \, \eta] \, d\eta \qquad (49)$$

since on DB Y(s) = γ (s). Substituting Equation (48) into (49) then yields

$$\psi(\mathbf{x},\mathbf{y}) = -\frac{4\mathbf{k}'}{\pi^2 \mathrm{bd}} \sum_{m=1}^{\infty} \sum_{n=0}^{\infty} \alpha n \frac{\cos \frac{n\pi \mathbf{x}}{\mathrm{b}} \sin \frac{m\pi \mathbf{y}}{\mathrm{d}}}{\frac{n^2}{\mathrm{b}^2} + \frac{m^2}{\mathrm{d}^2}} \cdot \left(50\right)$$

$$\int_{0}^{d} \cos \frac{n\pi \xi(\eta)}{\mathrm{b}} \sin \frac{m\pi \eta}{\mathrm{d}} d\eta.$$

If (50) is made dimensionless, we have

$$\Psi' = \frac{\Psi}{\frac{4k'd}{\pi^2}(\frac{b}{d})} = -\sum_{m=1}^{\infty} \sum_{n=0}^{\infty} \alpha_n \frac{\cos \frac{n\pi x}{b} \sin \frac{m\pi y}{d}}{n^2 + m^2(\frac{b}{d})^2}$$

$$\int_{0}^{1} \cos \frac{n\pi \xi}{b} \sin \frac{m\pi \eta}{d} d(\frac{\eta}{d}).$$
(51)

The function Ψ' in Equation (51) is computed numerically, and the movement of the interface is derived from it. A detailed account of the numerical solution is explained below. The Control Data 3600 Computer of the Michigan State University Computer Center was used for all the numerical computation. The computing procedures are as follows:

- 1) Assume an initial interface position DB.
- The interface position is expressed in the form of a group of discrete points (x_i, y_i). The intermediate points among these discrete points are computed by interpolation using Newton's

- divided difference formula. This formula is listed in Appendix II. These values are stored in the memory of the computer for later use.
- The integral in Equation (51) is evaluated along the interface using Simpson's rule with intervals of $\frac{\Delta \gamma}{d} = 0.001$. The results of part (2) are utilized in obtaining the values of $\frac{\xi}{d}$.
- 4) ψ in Equation (51) is then computed along the interface at the intervals of $\frac{\Delta y}{d}$ = 0.1 except the points near the end B where intervals of $\frac{\Delta y}{d}$ = 0.01 are used.
- 5) The numerical data giving ψ' at points on the interface is then differentiated with respect to dimensionless arc-length $\frac{s}{d}$ to obtain the normal velocity of particles on the interface.
- 6) The results of (5) are then multiplied by the dimensionless time increment $\frac{\Delta t k'}{d}$ to obtain the dimensionless displacement $\frac{\Delta n}{d}$ of the interface in the normal direction. The horizontal and vertical components of this displacement are obtained by multiplying $\frac{\Delta n}{d}$ by the direction cosines of the normal.
- 7) The new position of the interface is then obtained by adding these horizontal and vertical components of the normal displacement to the corresponding initial co-ordinates of the interface. (Note that these x and y components are not actual x and y

components of the displacement of material particles, since particles would also have some velocity components tangential to the interface, computed from the normal derivative of Ψ' and therefore discontinuous at the interface.)

- 8) These co-ordinates are then substituted again in Newton's divided difference interpolation formula to obtain the intermediate points.
- 9) Parts (2) through (8) are then repeated to obtain the subsequent positions of the interface.

In Appendix III, the entire computational schemes are presented in the form of Flow Diagrams so that the computer instructions can be easily programmed from them.

Two sample FORTRAN Programs are presented in Appendix IV for reference.

C. Numerical Example

For the purpose of illustration, a numerical example, with the following data is presented:

$$\frac{b}{d} = 20, \qquad \frac{k'd}{0} = 30.$$

The initial interface position was obtained from the equilibrium position calculated by Henry (1959) for a discharge rate represented by $\frac{\mathbf{k'd}}{\mathbf{Q}} = 40.025$. Co-ordinates of eleven points along the initial interface are shown in Table 5. Additional points on the interface were obtained by interpolation as described in step (2) of the procedure given in the preceding section. At time t = 0 it is

assumed that the discharge rate is suddenly increased and maintained during the transient motion of the interface at a rate represented by $\frac{\mathbf{k'd}}{Q} = 30$.

D. Results and Discussion

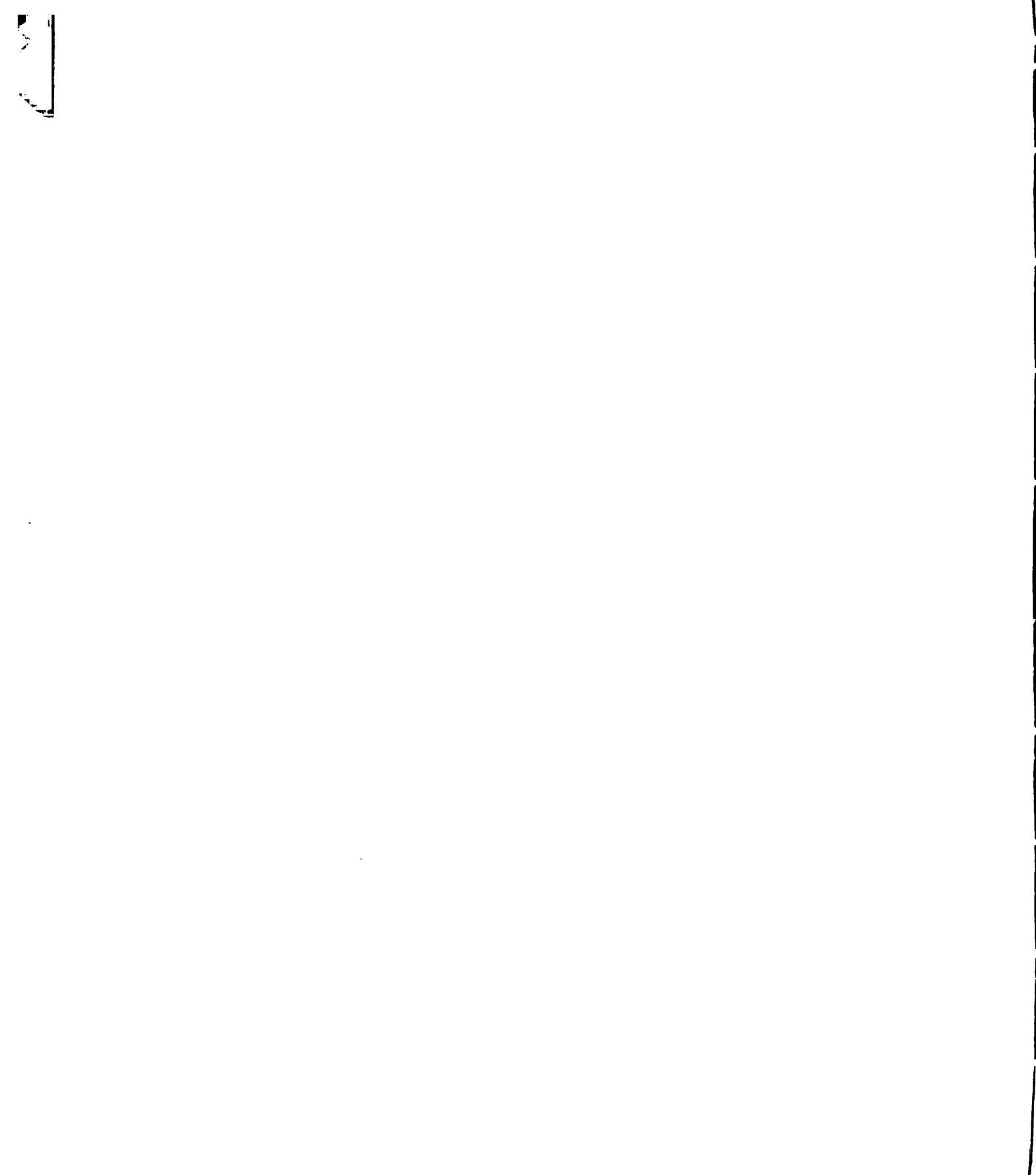
Table 4 shows the values of Ψ' (labeled PSI) between $\frac{Y}{d} = 0.1$ and $\frac{Y}{d} = 0.8$ along the initial interface, the results of step (4) of the first computation cycle. The number k in the table indicates the number of terms in the double series of Equation (51); thus k = 60 means a partial sum with m going from 1 to 60 while n goes from zero to 60, a total of 3,660 terms in the double sum. Since the results for k = 50 agree with those for k = 60 to approximately four significant figures, it is hoped that sufficient convergence was obtained to give results accurate to approximately four significant figures. This result is plotted in Figure 13, showing that the relation between Ψ' and $\frac{Y}{d}$ is linear except at the points beyond $\frac{Y}{d} = 0.80$, which are computed separately and given in Table 6.

Two cycles of the calculation outlined in part B were performed to obtain the interface positions at times corresponding to $\frac{tk'}{d}$ equal to ten and twenty. The resulting interface positions are plotted along with the initial interface position in Figure 14, based on Table 5, which gives the position co-ordinates of eleven points on the interface after the motion. It appears from Figure 14 that the motion during the second time increment was

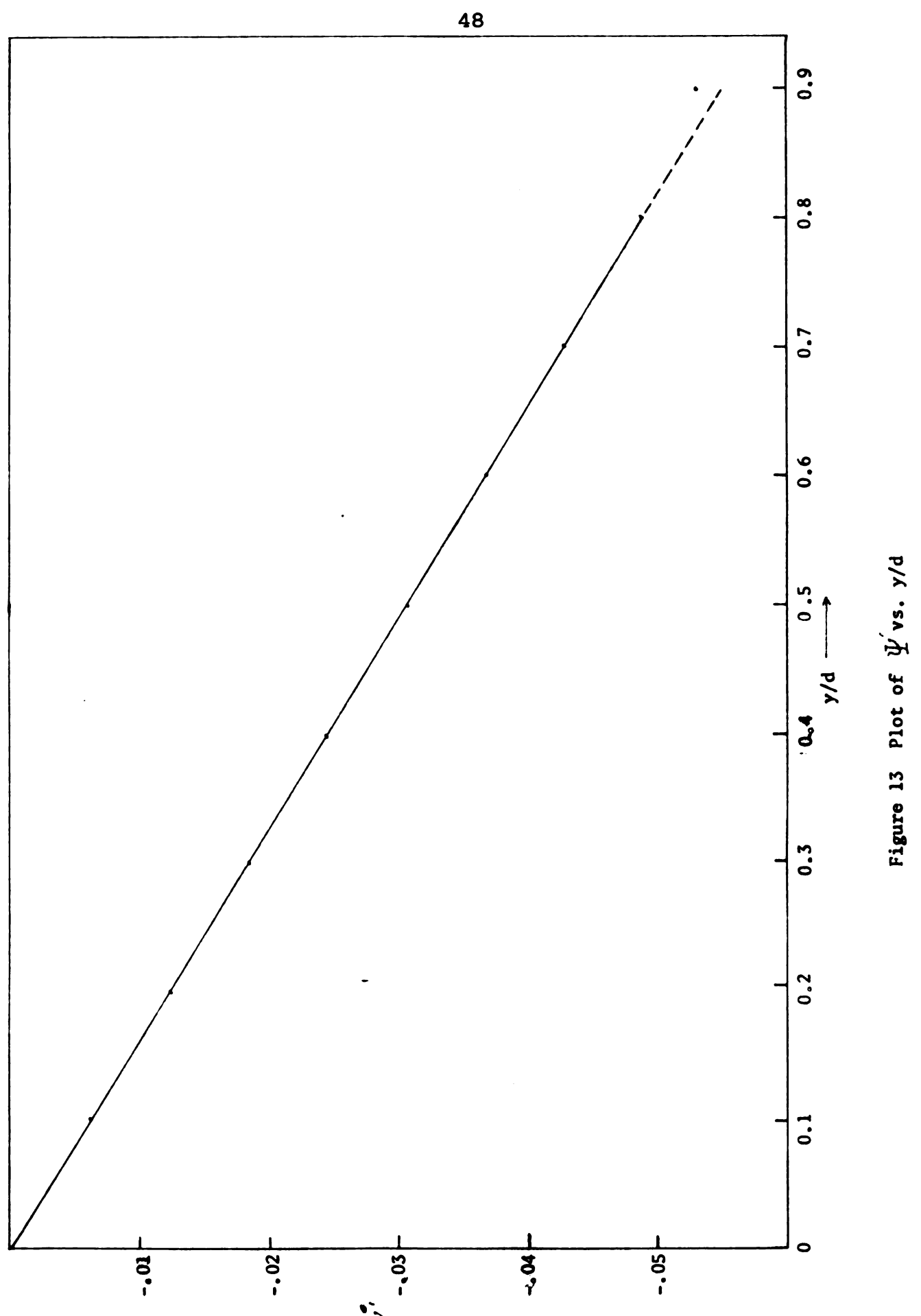
considerably smaller than during the first. This plot shows a more reasonable motion of the interface than was obtained by the one-dimensional analysis. However, a closer examination of the region near the right-hand end of the flow field shows still some discrepancy.

In the region between $\frac{Y}{d}=0.8$ and $\frac{Y}{d}=1$, the computations were performed at intervals $\frac{\Delta Y}{d}=0.01$. The results for ψ' are given in Table 6 with the series carried out to k=110 in order to get sufficient convergence. The results are also plotted in Figure 15, and it is seen that the linear plot of Figure 13 extends to about $\frac{Y}{d}=0.89$. Beyond this point the results become erratic and unreasonable. The position of the part of the interface between $\frac{Y}{d}=0.8$ and $\frac{Y}{d}=1$ after $\frac{tk}{d}=10$ is shown in Figure 16, based on Table 7. Near the right-hand end the large displacement shown is in the region where the solution is erratic. Perhaps a better result could be obtained by taking a smaller interval in the interpolation formula and the numerical integration.

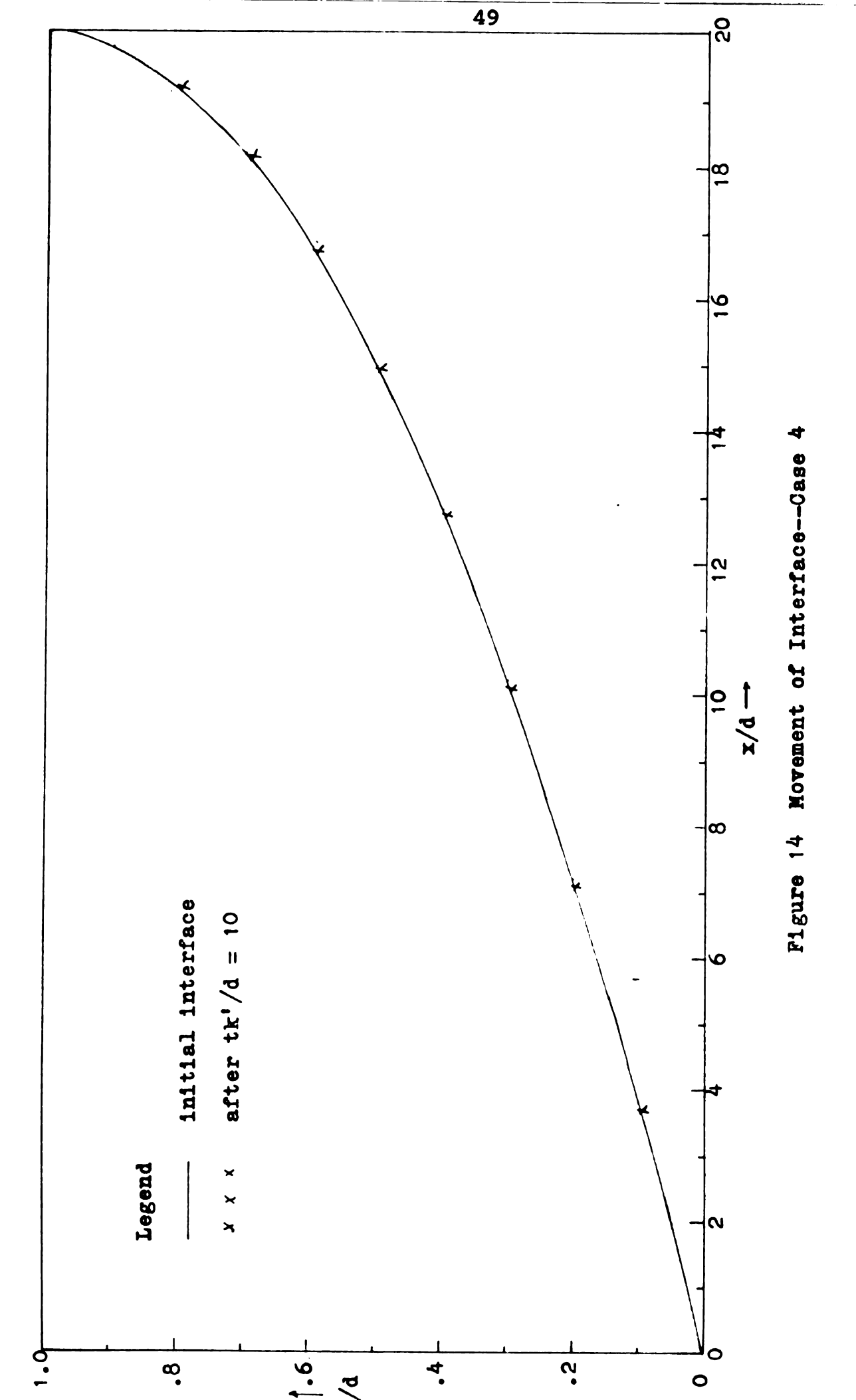
end, the two-dimensional analysis predictions seem reasonable, and the unreasonable behavior occurs in a much smaller part of the field than was the case with the one-dimensional analysis.











50

The state of the s

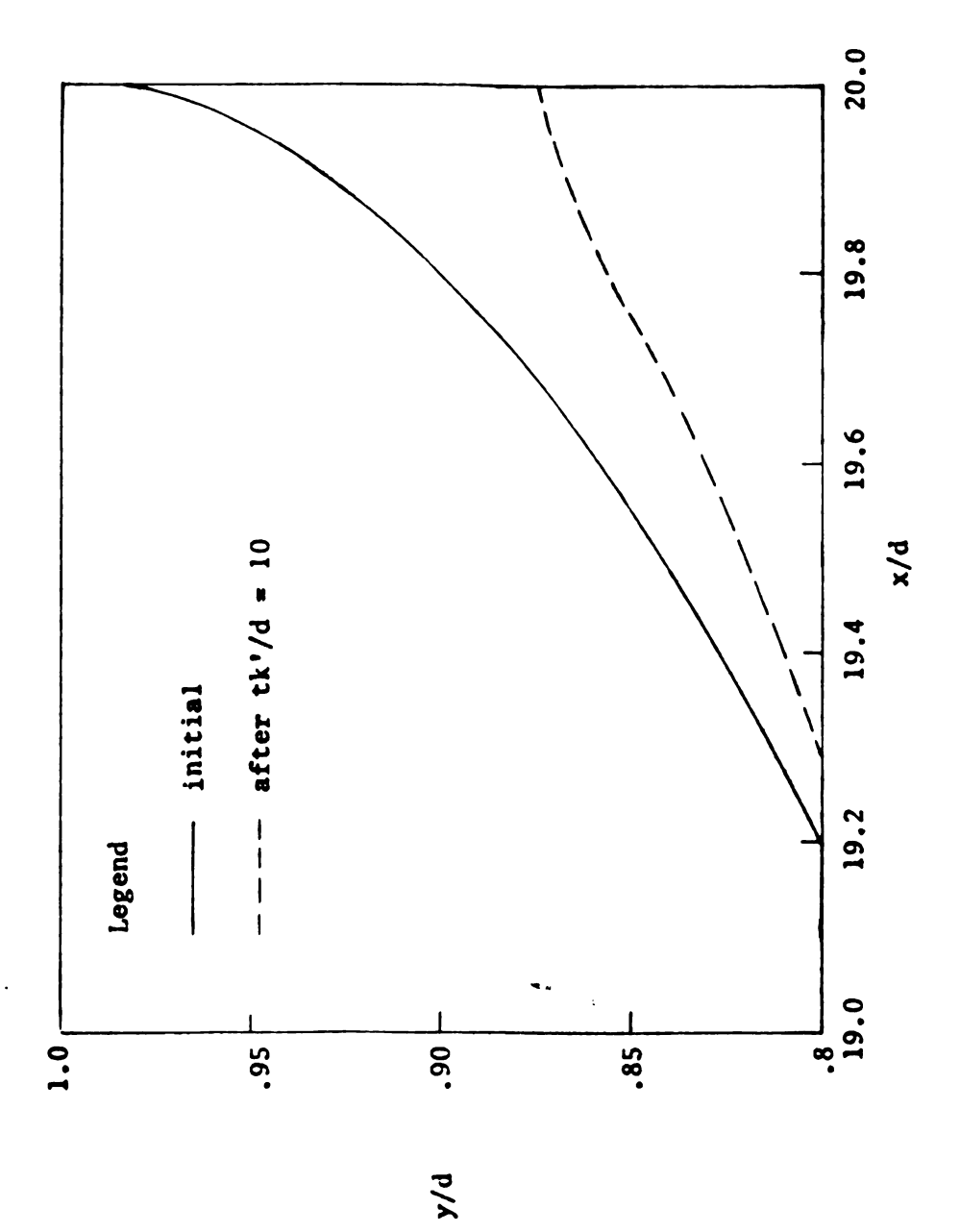


Figure 16 Movement of Interface -- Case 5

TABLE 4 VALUES OF PSI ALONG INITIAL INTERFACE FOR Y/D=0.1 TO 0.8

(TABULATION FOR FIGURE 13)

	Y/D	PSI	DIFFERENCE
K=10	0.10	-•553055545737E-02	553055545737E-02
	0.20	115720761094E-01	115720761094E-01
	0.30	176355510117E-01	176355510117E-01
	0.40	236459464657E-01	236459464657E-01
	0.50	295596062300E-01	295596062300E-01
	0.60	351179062585E-01	351179062585E-01
	0.70	398317114792E-01	398317114792E-01
	0.80	-•448916755369E-01	448916755369E-01
K=20	0.10	582795472379E-02	297369296528E-03
K-20	0.20	119473692097E-01	375293100216E-03
	0.20	-•180447219584E-01	-•409170946587E-03
	0.40	-•241584277297E-01	512481264217E-03
	0.50	-•301895540055E-01	629947775480E-03
	0.60	360999112490E-01	982004990918E-03
	0.70	414043748577E-01	-•157266337832E-02
	0.80	453687964662E-01	477120928750E-03
	0000	14330077043022 01	- 14//120920/302-03
K=30	0.10	594017702912E-02	112222305352E-03
	0.20	120689791407E-01	-•121609931060E-03
	0.30	181970215872E-01	152299629015E-03
	0.40	243173068215E-01	158879091 49 4E-03
	0.50	-•303962968195E-01	206742814506E-03
	0.60	363412571118E-01	-•241345862385E-03
	0.70	-•419695166318E-01	565141774161E-03
	0.80	-•471293439819E-01	-•176054751595E-02
K=40	0.10	599469170993E-02	545146807563E-04
	0.20	-•121334040316E-01	644248907542E-04
	0.30	182704867486E-01	734651612234E-04
	0.40	244030406335E-01	857338122863E-04
	0.50	305048160917E-01	108519272093E-03
	0.60	365143438139E-01	173086702496E-03
	0.70	422962561803E-01	326739548669E-03
	0.80	-•474693501048E-01	-•340006123239E-03
K=50	0.10	602848758412E-02	337958741744E-04
	0.20	121729893888E-01	395853574002E-04
	0.30	183163778540E-01	458911054018E-04
	0.40	244519188225E-01	488781888642E-04
	0.50	305669839261E-01	621678341326E-04
	0.60	366090105235E-01	946667096301E-04
	0.70	424703593511E-01	174103171055E-03
	0.80	477747216275E-01	305371522714E-03

TABLE 4--CONTINUED

	Y/D	PSI	DIFFERENCE
K=60	0.10	605041735282E-02	219297686504E-04
	0.20	121992332453E-01	262438561556E-04
	0.30	183459515629E-01	295737086170E-04
	0.40	244866174082E-01	346985852964E-04
	0.50	306114952320E-01	445113055328E-04
	0.60	366647209405E-01	557104167470E-04
	0.70	425997797727E-01	129420421224E-03
	0.80	481022714914E-01	327549862974E-03

NOTE K INDICATES THE NUMBER OF TERMS IN EQUATION (51). FOR EXAMPLE.

K=60 MEANS THAT 60X60=3600 TERMS ARE CARRIED OUT IN THE SUMMATION

TABLE 5 MOVEMENT OF INTERFACE POSITION--CASE 4 (TABULATION FOR FIGURE 14)

	Y/D	X/D
AT T=0	0.000 0.100 0.200 0.300 0.400 0.500 0.600 0.700 0.800 0.900 0.982	0.000 .380237352438E+01 .720449719549E+01 .102063710230E+02 .128079950071E+02 .150093691478E+02 .168104934459E+02 .182113678999E+02 .192119925101E+02 .198123672759E+02 .2000000000000E+02
AFTER T=10	22710731E-02 .97638290E-01 .19738456E 00 .29700272E 00 .39645103E 00 .49560301E 00 .59399079E 00 .70233221E 00 .81574804E 00	.61477886E-04 .36941965E 01 .71083374E 01 .10122245E 02 .12735916E 02 .14949369E 02 .16762655E 02 .18174974E 02 .19186239E 02

- NOTE ••• 1. THE DATA FOR SECOND SET OF VALUES (AFTER T= 10)

 CORRESPOND TO THE FIRST 9 VALUES IN THE

 FIRST SET (AT T = 0)
 - 2. CONTROL DATA 3600 WAS USED FOR T = 0 AND IBM 1620 WAS USED FOR T = 10

TABLE 6 VALUES OF PSI FOR INITIAL INTERFACE POSITION Y=0.810 TO 0.982 (TABULATION OF FIGURE 15)

	Y/D	PSI	DIFFERENCE
K= 10	.810	452184037582E-01	452184037582E-01
	.820	453708840054E-01	453708840054E-01
	•830	453144403000E-01	453144403000E-01
	.840	450179562191E-01	450179562191E-01
	.850	444540875447E-01	444540875447E-01
	.860	435993889711E-01	-•435993889711E-01
	•870	424344879320E-01	-•424344879320E-01
	.880	409443807417E-01	-•409443807417E-01
	•890	391188634036E-01	391188634036E-01
	•900	369530592252E-01	369530592252E-01
	•910	344483332432E-01	344483332432E-01
	•920	-•316116333968E-01	316116333968E-01
	•930	284569470103E-01	284569470103E-01
	•940	250050968927E-01	250050968927E-01
	•950	212836335268E-01	212836335268E-01
	•960	173264630052E-01	173264630052E-01
	•970	131732188562E-01	-•131732188562E-01
	•980	886840445251E-02	-•886840445251E-02
	•982	-•799351987516E-02	-•79935198751 6 E-02
K= 20	.810	457766126623E-01	558208904302E-03
	.820	463284042831E-01	-•957520277560E-03
	.830	469820578153E-01	166761751556E-02
	.840	476526464969E-01	263469027785E-02
	.850	482256676085E+01	377158006362E-02
	•860	485752950466E-01	-•497590607585E-02
	.870	485827919299E-01	614830399820E-02
	.880	481503599367E-01	720597919470E-02
	•890	472074536941E-01	808859029086E-02
	•900	-•457093757883E-01	-•875631656367E-02
	•910	436321422130E-01	-•918380896939E-02
	•920	-•409600791230E-01	-•934844572679E-02
	•930	376849203712E-01	922797336098E-02
	•940	338044417331E-01	879934483979E-02
	•950	293274613025E-01	804382777569E-02
	•960	242819787385E-01	695551573343E-02
	•970	187233390643E-01	555012020792E-02
	•980	127392746388E-01	387087018644E-02
	•982	-•115018000693E-01	350828019422E-02

TABLE 6--CONTINUED

	Y/D	PSI	DIFFERENCE
K= 30	.810	472920946682E-01	151548200578E-02
	.820	473523386812E-01	102393439831E-02
	.830	474514539543E-01	469396139124E-03
	.840	477125641155E-01	599176182746E-04
	.850	481861443230E-01	•39523285523 3 E-04
	. 860	488250453061E-01	249750259176E-03
	.870	494889206624E-01	906128732822E-03
	.880	499733504439E-01	182299050724E-02
	.890	500545813906E-01	284712769651E-02
	•900	495342207585E-01	382484497008E-02
	•910	482702450587E-01	463810284607E-02
	.920	461712520708E-01	521117294746E-02
	•930	431911012289E-01	550618085806E-02
	•940	393110517856E-01	550661005327E-02
	•950	345345048154E-01	520704351235E-02
	•960	288942944855E-01	461231574678E-02
	•970	224660673521E-01	374272828783E-02
	.980	153785767827E-01	263930214380E-02
	• 98 2	138980940221E-01	239629395270E-02
K= 40	.810	480871367705E-01	795042102254E-03
	.820	485735333459E-01	122119466416E-02
	.830	488033338195E-01	135187986511E-02
	.840	488194414735E-01	-•110687735834E-02
	.850	488097096510E-01	-•623565328176E-03
	.860	489774046000E-01	152359293683E-03
	.870	494171075858E-01	•718130768306E-04
	.880	500631167379E-01	897662939693E-04
	. 890	506948285052E-01	640247114468E-03
	•900	509814612364E-01	144724047826E-02
	•910	505792526834E-01	230900762475E-02
	•920	492239518324E-01	305269976168E-02
	•930	467835343385E-01	359243310966E-02
	•940	432035788072E-01	389252702102E-02
	•950	384418794943E-01	390737467940E-02
	•960	324799319184E-01	358563743255E-02
	•970	253981002330E-01	293203288136E-02
	•980	174167838861E-01	-•203820710343E-02
	•982	157412018762E-01	-•184310785382E-02

TABLE 6--CONTINUED

	Y/D	PSI	DIFFERENCE
K= 50	.810	481634665775E-01	763298066900E-04
	.820	487147646396E-01	141231294041E-03
	. 830	493299794303E-01	526645610997E-03
	.840	497661655689E-01	-•946724095236E-03
	.850	498873843368E-01	107767468582E-02
	.860	497962164540E-01	818811854522E-03
	.870	497808570639E-01	363749478318E-03
	.880	500798562876E-01	167395501197E-04
	. 890	506720480247E-01	•227804812315E-04
	•900	512978024577E-01	316341221158E-03
	•910	515718601426E-01	992607459018E-03
	.920	510197363445E-01	179578451211E-02
	•930	492309120069E-01	244737766847E-02
	•940	460339127058E-01	283033389867E-02
	•950	414321020340E-01	299022253974E-02
	•960	353883813827E-01	290844946452E-02
	•970	278702420605E-01	247214182724E-02
	.980	191220144316E-01	170523054523E-02
	•982	-•172729686939E-01	153176681808E-02
K= 60	.810	-•485827322533E-01	419265676101E-03
	.820	4 8 9249962920E-01	210231652090E-03
	.830	493560598668E-01	260804363286E-04
	.840	-•499627180303E-01	196552461603E-03
	.850	505022735364E-01	614889199831E-03
	.860	506885582625E-01	892341808139E-03
	.870	505629894935E-01	782132428867E-03
	.880	504551362523E-01	375279964835E-03
	•890	506928273040E-01	207792791120E-04
	•900	512968505820E-01	•951875335901E-06
	•910	518915871333E-01	319726990718E-03
	•920	519284426817E-01	908706337214E-03
	•930	508612640420E-01	163035203517E-02
	•940	482110196281E-01	217710692235E-02
	•950	438177780175E-01	-•238567598357E-02
	•960	377589277676E-01	237054638459E-02
	•970	-•299859439787E-01	211570191826E-02
	•980	206186886688E-01	149667423742E-02
	•982	186147186814E-01	134174998722E-02

TABLE 6--CONTINUED

	Y/D	PSI	DIFFERENCE
K= 70	.810	487233091830E-01	140576929884E-03
	.820	492770942314E-01	352097939875E-03
	.830	-•496358667209E-01	279806854458E-03
	.840	500081645529E-01	454465225637E-04
	.850	~•505883439895E-01	86070452199 8 E-04
	.860	511448045057E-01	456246243630E-03
	.870	513168679303E-01	753878436633E-03
	.880	511243153218E-01	-•669179069533E-03
	•890	509902017104E-01	297374407644E-03
	•900	512766537460E-01	•201968368860E-04
	•910	519274954102E-01	359082769144E-04
	•920	523762289595E-01	-•447786277618E-03
	•930	518802227132E-01	-•101895867103E-02
	•940	498314128214E-01	162039319370E-02
	•950	458036090546E-01	198583103705E-02
	•960	397633889501E-01	200446118291E-02
	•970	317970749391E-01	-•181113096009E+02
	•980	219485890513E-01	132990038266E-02
	•982	198128739656E-01	1198155284 35E-0 2
K= 80	.810	488057376664E-01	824284834394E-04
	.820	493395512865E-01	624570548112E-04
	.830	499160038438E-01	280137122907E-03
	.840	502793829161E-01	271218363203E-03
	.850	506330617296E-01	447177408212E-04
	.860	512172595030E-01	724549 96 3721E-04
	.870	517383527884E-01	421484858634E-03
	.880	517916155295E-01	667300207177E-03
	.890	515100689212E-01	519867210649E-03
	•900	514382958980E-01	161642152310E-03
	•910	518859315431E-01	•415638678540E-04
	•920	525279511159E-01	151722156264E-03
	•930	525285820899E-01	648359377024E-03
	•940	510266760015E-01	119526317942E-02
	•950	474280648501E-01	162445579557E-02
	•960	415139840159E-01	175059506550E-02
	•970	333831410448E-01	158606610607E-02
	•980	231252241239E-01	117663507264E-02
	•982	208794458089E-01	106657184326E-02

TABLE 6--CONTINUED

	Y/D	PSI	DIFFERENCE
K= 90	.810	490242524080E-01	218514741391E-03
	.820	494326401109E-01	930888245435E-04
	.830	499569622698E-01	409584254165E-04
	.840	505279814039E-01	248598487819E-03
	.850	508639785854E-01	230916855799E-03
	.860	512372014171E-01	199419146160E-04
	.870	518449229319E-01	106570143544E-03
	.880	522450445671E-01	453429037407E-03
	•890	520947900208E-01	584721099600E-03
	•900	517758752758E-01	337579377636E-03
	•910	519113687056E-01	254371625495E-04
	•920	525386022244E-01	106511088235E-04
	•930	528972172862E-01	368635195635E-03
	•940	519190544233E-01	-•892378422577E-03
	•950	487641899512E-01	133612510130E-02
	•960	430385188425E-01	152453482682E-02
	•970	348078925490E-01	142475150373E-02
	•980	241740687696E-01	104884464556E-02
	•982	218306809391E-01	-•951235130298E-03
K=100	.810	490703423842E-01	460899764228E-04
	.820	-•496302525367E-01	197612425836E-03
	.830	500297199484E-01	727576789373E-04
	.840	505769080846E-01	-•489266803932E-04
	•850	511102328077E-01	246254222478E-03
	.860	514012544823E-01	164053064513E-03
	.870	518433598423E+01	•156308942678E-05
	.880	524399327172E-01	194888150872E-03
	.890	525873816587E-01	-•492591637347E-03
	•900	522253125819E-01	449437306088E-03
	•910	520503985230E-01	139029818460E-03
	•920	525071716605E-01	•314305634682E-04
	•930	530854861470E-01	188268861169E-03
	•940	525663235152E-01	-•647269092049E-03
	•950	498755067463E-01	1111316794B0E-02
	•960	443733745582E-01	133485571590E-02
	•970	360955859047E-01	128769335610E-02
	•980	251251792681E-01	-•951110498601E-03
	•982	226889534304E-01	858272491314E-03

TABLE 6--CONTINUED

	Y/D	PSI	DIFFERENCE
K=110	.810	491299317750E-01	595893907317E-04
	.820	496833540572E-01	531015202811E-04
	.830	502089331203E-01	179213171581E-03
	.840	506107013513E-01	337932669943E-04
	.850	511997619338E-01	895291259454E-04
	.860	516395901053E-01	238335624090E-03
	.870	519187912083E-01	754313659869E-04
	.880	524676420639E-01	277093458870E-04
	.890	529053012535E-01	317919594643E-03
	•900	526936291033E-01	468316521619E-03
	.910	522959259382E-01	245527414339E-03
	•920	525058360916E-01	•133556932273E-05
	•930	531482673861E-01	627812387407E-04
	•940	530391057327E-01	472782217003E-03
	•950	507855853444E-01	910078598288E-03
	•960	455636362247E-01	119026166614E-02
	•970	372563408215E-01	116075491680E-02
	•980	260020843823E-01	876905114186E-03
	•982	234770094637E-01	788056033343E-03

-		
-		
-		
	-	
· · · · · · · · · · · · · · · · · · ·		
, ;		! !

TABLE 7 MOVEMENT OF INTERFACE POSITION-→CASE 5 (TABULATION FOR FIGURE 16)

	Y/D		X/D
AT T=0	0.800 0.810 0.820 0.830 0.840 0.850 0.860 0.870 0.880 0.990 0.910 0.920 0.930 0.940 0.950 0.960 0.970 0.980 0.982		•19211993E+02 •19290055E+02 •19364119E+02 •19434183E+02 •19500247E+02 •19562308E+02 •19620362E+02 •19674405E+02 •19724427E+02 •19770419E+02 •19812367E+02 •19850391E+02 •19850391E+02 •19984412E+02 •19944431E+02 •19962461E+02 •19980472E+02 •19994481E+02 •20004487E+02 •20000000E+02
AFTER T=10	.79570146E .80075022E .80438676E .80908718E .81980150E .82977453E .82977453E .82755685E .83931947E .85336304E .82782176E .79248004E .81427781E .87429744E .85868187E .65180278E .21100515E -42161320E -11432038E -91320570E .30086771E	00 00 00 00 00 00 00 00 00 00 00 00 00	•19212544E 02 •19291271E 02 •19366286E 02 •19437256E 02 •19503400E 02 •19565676E 02 •19626150E 02 •19680301E 02 •19729976E 02 •19729976E 02 •19784560E 02 •19839256E 02 •19876964E 02 •19898685E 02 •19939886E 02 •20060454E 02 •20331728E 02 •20843441E 02 •24120897E 02 •24120897E 02

NOTE ... IBM 1620 WAS USED FOR THE COMPUTATION.

• •

. .

CHAPTER IV

CONCLUSION

This thesis has presented an analytical method by which the movement of the interface for transient twophase flow in a porous medium can be predicted. Darcy's
law is a well-established fundamental principle based
upon which all problems concerning the flow through porous
media are formulated. The use of Darcy's law in this continuity equation then yields Laplace's equation, and the
resulting boundary value problem is solved.

Two approaches are used in solving the problem.

The first of these is to consider the flow as one
dimensional while the other is to consider the flow as

two-dimensional.

The results of the one-dimensional analysis are represented by Figures 5 through 8. These results indicate that the velocity near the outflow seepage face cannot be approximated by the one-dimensional assumption, and the need for two-dimensional analysis is necessary.

In the beginning of this investigation, the relaxation method was tried in solving the two-dimensional problem. However, it was found that this method would be unsuitable, if not impossible, for use with digital

computer, because the relaxation patterns in the vicinity of the interface change with the movement of the interface. This has led to the adoption of the present method. The results, as are represented by Figures 13 through 16, make available an analytical method which can be compared with field measurements and model tests. Although two different sets of data are used in the two approaches, the results are qualitatively the same except near the outflow seepage face. Comparison of Figures 8 and 16 reveals that while in the one-dimensional analysis reasonable results are obtained up to about $\frac{\mathbf{x}}{\mathbf{d}} = 2$ from the end, a reasonable result is obtained up to about $\frac{\mathbf{x}}{\mathbf{d}} = 0.1$ in the two-dimensional analysis.

The digital computer is utilized only for the two-dimensional analysis. The computation time for obtaining the results shown in Table 4 was about 60 minutes, while for Table 6 it was 160 minutes. For Tables 5 and 7, the time was just a fraction of a minute. It appears, therefore, that a computer which equals or excels Control Data 3600 in processing speed should be used.

The method presented here can be applied to the problem with an initial interface of arbitrary shape. It can also be applied, with some modification, to the problem with different geometry. The problem in which the compressibility of fluids is taken into account and the effect of miscibility on the flow field present other possibilities for future study.

BIBLIOGRAPHY

- 1. Badon-Ghyben, W. Nota in verband met de voorgenomen putboring nabij Amsterdam, <u>Ingenieur</u>, <u>Utrecht</u>, p. 21, 1888-89.
- 2. Bear, J. and Dagon, G. Moving Interface in Coastal Aquifers, <u>Journal of Hydraulics Division</u>, Vol. 90, No. HY4, July, 1964, p. 193. American Society of Civil Engineers.
- 3. Collins, R. E. Flow of Fluids through Porous Materials, Reinhold, New York, 1961.
- 4. Coats, K. H. Unsteady-State Liquid Flow through Porous Media Having Elliptic Boundaries, Petro-leum Transactions, AIME, T.N. 2050, Vol. 216, 1959.
- 5. DeJong DeJosselin, G. Singularity Distributions for the Analysis of Multiple-Fluid Flow through Porous Media, <u>Journal of Geo-physical Research</u>, Vol. 65, No. 11, 1960.
- 6. DeWiest, R. J. M. Unsteady-state Phenomena in Flow through Porous Media, <u>Technical Report</u>, No. 3, Department of Civil Engineering, Stanford University, 1959.
- 7. Dupuit, J. Etudes theoriques et pratiques sur le mouvementdes eaux a travers les terrains permeables, Carilian-Goeury, Paris, 1863.
- 8. Forchheimer, Ph. Zeits Arch. Ing. Ver. Hannover, 1886.
- 9. Henry, H. R. Salt Intrusion into Fresh-water Aquifers, <u>Journal of Geophysical Research</u>, Vol. 64, No. 11, 1959.
- 10. Herzberg, B. Die Wasserversorgung einiger Nordseebader, J. Gasbeleuchtung and Wasserversorgung, 44, 815-19, 842-44, 1901.
- 11. Hubbert, K. Darcy's Law and the Field Equations of the Flow of Underground Fluids, <u>Journal of Petroleum Technology</u>, October, 1956.

- 12. Hubbert, M. K. The Theory of Ground-water Motion, Journal of Geology, 48, 785-944, 1940.
- 13. Jacob, C. E. Flow of Ground Water, Chapter V,

 Engineering Hydraulics, edited by H. Rouse, John
 Wiley, New York, 1950.
- 14. Kidder, R. E. Flow of Immiscible Fluids in Porous Media: Exact Solution of a Free Boundary Problem, Journal of Applied Physics, Vol. 27, No. 8, 1956.
- 15. Kidder, R. E. Motion of the Interface between Two Immiscible Liquids of Unequal Density in a Porous Solid, <u>Journal of Applied Physics</u>, Vol. 27, No. 12, 1956.
- 16. Kitagawa, K. Un aspect du develloppement des etudes des eaux soutteraines au Japon, <u>Japanese</u>
 <u>Journal of Astronomy and Geophysics</u>, 17, 141-55, 1939.
- 17. Kunz, Kaiser S. Numerical Analysis, McGraw Hill, New York, 1957.
- 18. Muskat, M. The Flow of Homogeneous Fluids through Porous Media, J. W. Edwards, Ann Arbor, 1946.
- 19. Scheidegger, A. The Physics of Flow through Porous Media, Macmillan, New York, 1957.
- 20. Todd, D. K. Sea Water Intrusion in Coastal Aquifers, <u>Transactions, American Geophysical Union</u>, Vol. 34, No. 5, 1953.

APPENDIX I

LIST OF SYMBOLS

The following symbols are used throughout this thesis:

Symbol	Definition	Dimension
^a 1, ^a 2	surface levels of liquid reservoir	L
b	length of porous medium	L
d	depth of porous medium	L
f(t)	some function of time	
g	acceleration due to gravity	L/T ²
h,h ₁ ,h ₂	piezometric head	L
ĵ	unit vector in the vertical direction	
К	permeability of porous medium	L ²
k, k_1, k_2	hydraulic conductivity	L/T
k'	<pre>product of hydraulic conductivity and buoyancy</pre>	L/T
m,n	integers	
ⁿ 1, ⁿ 2	normals to a surface	
p	pressure in fluid	F/L ²
Q	discharge per unit width in porous medium	L ² /T
\overrightarrow{q}	local velocity vector	L/T
s	distance along the interface	L
t	time	т

Symbol	Definition	Dimension
u,u ₁ ,u ₂	\mathbf{x} components of \overrightarrow{q}	L/T
	y components of \overrightarrow{q}	L/T
x	horizontal co-ordinate	L
Y	vertical co-ordinate of interface	L
У	vertical co-ordinate	L
$\gamma, \gamma_1, \gamma_2$	specific weights of fluids	F/L ³
Γ	$=\frac{\gamma_2-\gamma_1}{\gamma_1}$	
P	density of fluid	M/L ³
P(\$,7)	intensity of source	
*	horizontal co-ordinate along interface	L
7	vertical co-ordinate along interface	L
Ψ	modified stream function	L ² /T
ψ	stream function	L ² /T
$\varphi, \varphi_1, \varphi_2$	velocity potentials	L ² /T
θ	porosity of porous medium	
M	viscosity of fluid	M/LT
G()	Green's function	
() _x etc.	partial derivatives of a function () with respect to \mathbf{x} , etc.	
∇^2	Laplacian operator	

APPENDIX II

FORMULAS USED IN NUMERICAL APPROXIMATION

A. Newton's Divided-difference Interpolation Formula

$$\mathbf{x} = \mathbf{f}(\mathbf{y}) = \mathbf{f}(\mathbf{y}_{0}) + (\mathbf{y} - \mathbf{y}_{0})\mathbf{f}(\mathbf{y}_{0}, \mathbf{y}_{1}) + (\mathbf{y} - \mathbf{y}_{0})(\mathbf{y} - \mathbf{y}_{1}) *$$

$$\mathbf{f}(\mathbf{y}_{0}, \mathbf{y}_{1}, \mathbf{y}_{2}) + (\mathbf{y} - \mathbf{y}_{0})(\mathbf{y} - \mathbf{y}_{1})(\mathbf{y} - \mathbf{y}_{2})\mathbf{f}(\mathbf{y}_{0}, \mathbf{y}_{1}, \mathbf{y}_{2}, \mathbf{y}_{3}) +$$

$$\cdot \cdot \cdot + (\mathbf{y} - \mathbf{y}_{0})(\mathbf{y} - \mathbf{y}_{1}) \cdot \cdot \cdot (\mathbf{y} - \mathbf{y}_{n-1})\mathbf{f}(\mathbf{y}_{0}, \mathbf{y}_{1},$$

$$\cdot \cdot \cdot \mathbf{y}_{n})$$

where $f(y_0,y_1)$, $f(y_0,y_1,y_2)$. . . etc. are the divided differences of f(y) defined as

$$f(y_0, y_1) = \frac{f(y_0) - f(y_1)}{y_0 - y_1}$$

$$f(y_0, y_1, y_2) = \frac{f(y_0, y_1) - f(y_1, y_2)}{y_0 - y_2}$$

$$f(y_0, y_1, y_2, ..., y_n) =$$

$$\frac{f(y_0,y_1,y_2,\ldots,y_{n-1})-f(y_1,y_2,\ldots,y_n)}{y_0-y_n}.$$

B. Simpson's One-third Rule for Numerical Integration

$$\int_{a}^{b} f(x)ds = \frac{h}{3}(f_0 + 4f_1 + 2f_2 + 4f_3 + 2f_4 + \cdots$$

$$4f_{N-1} + f_N)$$

where $h = \frac{b - a}{N}$.

C. Numerical Differentiation Formulas

$$\frac{\mathrm{d}\mathbf{y}}{\mathrm{d}\mathbf{x}}\mathbf{1}_{\mathbf{x}=\mathbf{x}_{n}} \cong \frac{\mathbf{y}_{n+1} - \mathbf{y}_{n-1}}{\mathbf{x}_{n+1} - \mathbf{x}_{n-1}}$$

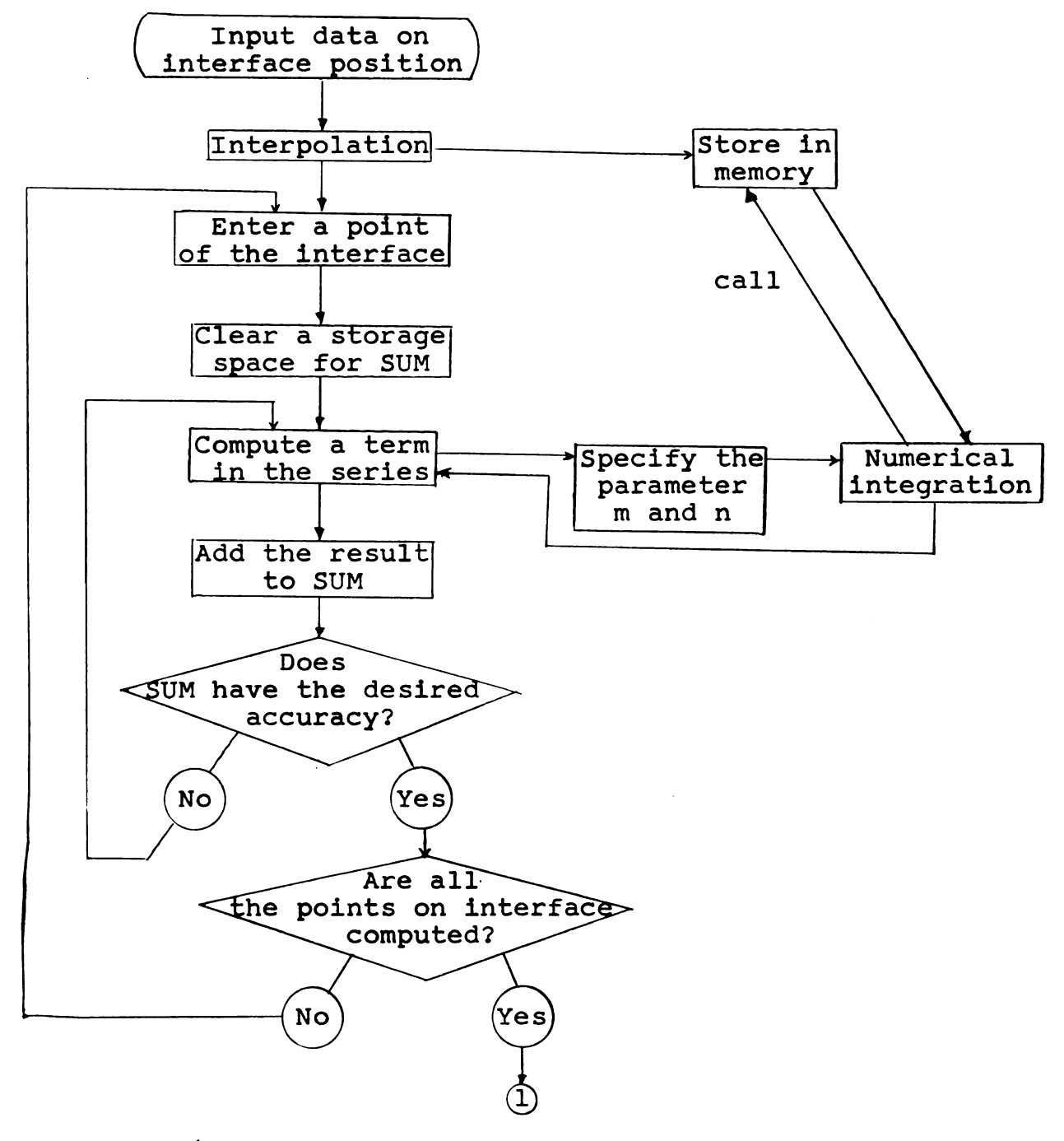
if $x \neq x_0$, $x \neq x_N$ where N is the end point, n = 0 and n = N.

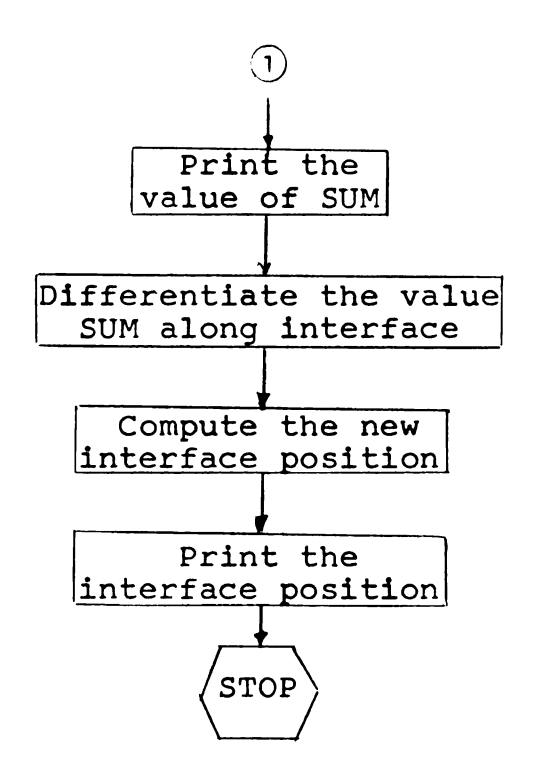
$$\frac{\mathrm{d}\mathbf{y}}{\mathrm{d}\mathbf{x}}]_{\mathbf{x}=\mathbf{x}_0} \cong \frac{\mathbf{y}_1 - \mathbf{y}_0}{\mathbf{x}_1 - \mathbf{x}_0}$$

$$\frac{\mathrm{d}\mathbf{y}}{\mathrm{d}\mathbf{x}}]_{\mathbf{x}=\mathbf{x}_{\mathrm{N}}} \cong \frac{\mathbf{y}_{\mathrm{N}} - \mathbf{y}_{\mathrm{N}-1}}{\mathbf{x}_{\mathrm{N}} - \mathbf{x}_{\mathrm{N}-1}}.$$

APPENDIX III

FLOW CHART FOR COMPUTATION





Repeat the process as desired

APPENDIX IV

SAMPLE FORTRAN PROGRAMS

Two sample FORTRAN programs, without input data, are presented here. Comment statements are inserted wherever necessary to interprete the sequences of FORTRAN statements.

PROGRAM PSI executes the computation of Equation (51) and the steps (1) through (4) as is indicated in Chapter III.

PROGRAM NEW POSN carries out the computation of a new interface position as is indicated by steps (5) through (7) in Chapter III.

Although these FORTRAN programs are written exclusively for execution by a Control Data 3600 computer, they can also be used for any other computer adopting the standard FORTRAN language.

```
PROGRAM PSI
C COMPUTATION OF PSI ALONG THE INTERFACE
      FORMAT(5X+1HY+15X+3HPSI+17X+10HDIFFERENCE/)
 101
 102
      FORMAT(1H0.E8.2.5X.E18.12.5X.E18.12)
 103
      FORMAT(/1H0,2HK=,14/)
 110
     FORMAT(4(E18.12.1X))
 123
      FORMAT(2X.E18.12.2X.E18.12)
 125
     FORMAT(////)
      DIMENSION Y(21) . X(21) . PSI(21) . XPRIME(21) . YPRIME(21) . XBAR(1000)
      DIMENSION
                              DIV1(11) • DIV2(10) • DIV3(9) • DIV4(8) • DIV5(7) • DI
     1V6(6) • DIV7(5) • DIV8(4) • DIV9(3) • DIV10(2)
      DIMENSION SUM1(20), SUM2(20), DIFFC(20),
                                                            SIGMA (61.61)
C INPUT OF THE INTERFACE DATA
      READ 123. (Y(I).X(I).I=1.8)
C THE FOLLOWING STATEMENT STARTS THE EXECUTION OF INTERPOLATION PROCESS
      DO 150 I1=1.11
 150
      DIV1(I1)=0.0
      DO 151 12=1.10
 151
      D1V2(12)=0.0
      DO 152 I3=1.9
 152
      DIV3(13)=0.0
      DO 153 I4=1.8
 153
      DIV4(I4)=0.0
      DO 154 I5=1.7
 154
      DIV5(15)=0.0
      DO 155 16=1.6
 155
      DIV6(16)=0.0
      DO 156 17=1.5
 156
      DIV7(17)=0.0
      DO 157 I8=1.4
 157
      DIV8(18)=0.0
      DO 158 19=1.3
 158
      DIV9(19) = 0.0
      DO 159 I10=1.2
 159
      DIV10(I10)=0.0
      DO 165 JBAR=1,1000
 165
      XBAR (JBAR) = 0.0
      I = 1
      I1=1
 1
      DIV1(I1) = (X(I+1)-X(I))/(Y(I+1)-Y(I))
      I = I + 1
      I1 = I1 + 1
      IF(I-10)1.1.21
 21
      I = 1
      I1=1
      12=1
 2
      DIV2(I2) = (DIV1(I1+1) - DIV1(I1))/(Y(I+2) - Y(I))
      I=I+1
      I1 = I1 + 1
      12=12+1
      IF(I-9)2.2.31
 31
      I = 1
      12=1
      13=1
```

```
3
      DIV3(13) = (DIV2(12+1) - DIV2(12))/(Y(1+3) - Y(1))
      I = I + 1
      12=12+1
      13=13+1
      IF(I- 8)3.3.41
41
      I = 1
      13=1
      I4=1
      DIV4(I4) = (DIV3(I3+1) - DIV3(I3))/(Y(I+4) - Y(I))
      I = I + 1
      13=13+1
      14=14+1
      IF(I- 7)4,4,51
51
      I = 1
      [4=1
      15=1
5
      DIV5(I5) = (DIV4(I4+1) - DIV4(I4))/(Y(I+5) - Y(I))
      I = I + 1
      14=14+1
      15=15+1
      IF(I- 6)5.5.61
61
      I = 1
      15=1
      16=1
6
      DIV6(16) = (DIV5(15+1) - DIV5(15))/(Y(1+6) - Y(1))
      I = I + 1
      15=15+1
      16=16+1
      IF(I-5)6.6.71
71
      I = 1
      16=1
      17 = 1
7
      DIV7(I7) = (DIV6(I6+1)-DIV6(I6))/(Y(I+7)-Y(I))
      I = I + 1
      16=16+1
      17=17+1
      IF(1-4)7.7.81
81
      I = 1
      17=1
      18=1
      DIV8(18) = (DIV7(17+1) - DIV7(17))/(Y(1+8) - Y(1))
8
      I = I + 1
      17 = 17 + 1
      18=18+1
      IF(1-3)8.8.91
91
      I = 1
      18=1
      DIV9(19) = (DIV8(18+1) - DIV8(18))/(Y(1+9) - Y(1))
      I=I+1
      18=18+1
      19=19+1
      IF(1-2)9,9,1001
1001 I=1
```

```
19=1
      110=1
10
      DIV10(110) = (DIV9(19+1) - DIV9(19))/(Y(1+10) - Y(1))
      I = I + 1
      19=19+1
      110=110+1
      IF(I-1)10+10+16
16
      YBAR=0.001
      JBAR=1
17
      XBAR(JBAR)=X(1)
      PROD=(YBAR-Y(1))
      XBAR(JBAR)=XBAR(JBAR)+PROD*DIV1(1)
      PROD=PROD*(YBAR-Y(2))
      XBAR(JBAR)=XBAR(JBAR)+PROD*DIV2(1)
      PROD=PROD*(YBAR-Y(3))
      XBAR(JBAR)=XBAR(JBAR)+PROD*DIV3(1)
      PROD=PROD*(YBAR-Y(4))
      XBAR(JBAR)=XBAR(JBAR)+PROD*DIV4(1)
      PROD=PROD*(YBAR-Y(5))
      XBAR (JBAR) = XBAR (JBAR) + PROD*DIV5(1)
      PROD=PROD*(YBAR-Y(6))
      XBAR(JBAR)=XBAR(JBAR)+PROD*DIV6(1)
      PROD=PROD*(YBAR-Y(7))
      XBAR(JBAR)=XBAR(JBAR)+PROD*DIV7(1)
      PROD=PROD*(YBAR-Y(8))
      XBAR(JBAR)=XBAR(JBAR)+PROD*DIV8(1)
      PROD=PROD*(YBAR-Y(9))
      XBAR(JBAR)=XBAR(JBAR)+PROD*DIV9(1)
      PROD=PROD*(YBAR-Y(10))
      XBAR(JBAR)=XBAR(JBAR)+PROD*DIV10(1)
      YBAR=YBAR+0.001
      JBAR=JBAR+1
      IF(JBAR-1000)17.17.1698
1698 PRINT 110 + (XBAR (JBAR) + JBAR = 1
                                      ·1000)
      PUNCH 110 . (XBAR (JBAR) . JBAR=1
                                      ·1000)
WITH THE ABOVE STATEMENT THE INTERPOLATION PROCESS IS COMPLETED AND THE VALUE
 OF XBAR(
            ) ARE STORED
THE FOLLOWING STATEMENT STARTS THE SUMMATION OF SERIES
      DO 164 IBAR=1.20
      SUM1 (IBAR)=0.0
      SUM2 ( IBAR ) = 0 . 0
164
      DIFFC(IBAR)=0.0
      DO 166 M=1.121
      DO 166 NA=1+121
166
      SIGMA(M.NA)=0.0
      PRINT 125
      PRINT 101
      ASPECT=20.0
      SUM=0.0
```

PSUM=0.0 ASUM=0.0 K=10

GOTO 1734

```
1699 DO 1770 M=1,M5
      DO 1760 NA=N4 N5
      N=NA-1
 1700 IF(N)1701+1701+1702
 1701 ALPHA=0.5
      GOTO 1703
 1702 ALPHA=1.0
 1703 FM=M
      B=ALPHA*COSF(FN*3.1415927*XBAR(JBAR)/ASPECT)
      DENO=FN#FN+FM#FM#ASPECT#ASPECT
      B=B/DENO
      IF(IBAR-1)1756,1704,1756
C THE FOLLOWING STATEMENT STARTS THE NUMERICAL INTEGRATION
 1704 SIGMA(M.NA)=0.0
      C=4.0
      JBAR1=JBAR
      DO 1714 L=1.982
      FL=L
      YBAR1=FL/1000.
      TERM1=C*COSF(FN*3.1415927*XBAR(JBAR)/ASPECT)
      TERM1=TERM1*SINF(FM*3.1415927*YBAR1)
      IF(C-4.0)1712.1710.1712
 1710 C=2.0
      GOTO 1714
 1712 C=4.0
 1714 SIGMA(M.NA)=SIGMA(M.NA)+TERM1
      JBAR=JBAR1
      M3=M/2
      M2=M3*2
      IF (M2-M) 1751 + 1750 + 1751
 1750 TERM2=1.0-COSF(0.982*FM*3.1415926536)
      GOTO 1752
 1751 TERM2=-1.0-COSF(0.982*FM*3.1415926536)
 1752 N2=(N+1)/2
      N3=N2*2
      IF(N3-N-1)1754,1753,1754
 1753 TERM2=TERM2/(FM#3.1415926536)
      GOTO 1755
 1754 TERM2=(-TERM2)/(FM+3.1415926536)
 1755 SIGMA(M.NA)=SIGMA(M.NA)+TERM2
      SIGMA(M.NA)=SIGMA(M.NA)*0.001/3.0
C WITH THE ABOVE STATEMENT. THE NUMERICAL INTEGRATION IS COMPLETED
 1756 TERM=B*SIGMA(M.NA)
      SUM=SUM+TERM
 1760 CONTINUE
 1716 A=SINF(FM*3.1415927*YBAR)
      PSUM=A*SUM
      ASUM=ASUM+PSUM
      SUM=0.0
      IF(M-K1)1770+1765+1765
 1765 N4=1
 1770 CONTINUE
```

```
1724 PSI=(-1.0) *ASPECT*ASUM
      SUM1 (IBAR) = SUM1 (IBAR) + PSI
WITH THE ABOVE STATEMENTATHE SUMMATION OF SERIES IS COMPLETED AND VALUE OF P
 COMPUTED
      DIFFC(IBAR)=SUM1(IBAR)-SUM2(IBAR)
      SUM2(IBAR)=SUM1(IBAR)
      IF(IBAR- 1)1728,1726,1728
1726 PRINT 103.K
1728 PRINT 102 . YBAR . SUM1 (IBAR) . DIFFC (IBAR)
      PUNCH 123.SUM1(IBAR).SUM2(IBAR)
      YBAR=YBAR+0.1
      IBAR=IBAR+1
      JBAR=JBAR+100
      ASUM=0.0
      SUM=0.0
      IF(IBAR- 8)1730.1730.1732
1780 YBAR=0.982
      1BAR=19
      JBAR=982
      ASUM=0.0
      SUM=0.0
      GOTO 1730
1730 IF(K-10)1699.1699.1731
1731 N4=K1+2
      GOTO 1699
1732 K=K+10
      IF(K- 60)1734.1734.1736
1734 YBAR=0.10
      IBAR=1
      JBAR=100
      M5=K
      N5=K+1
      K1=K-10
      IF(K1)1737,1737,1735
1735 N4=K1+2
      GOTO 1699
1737 N4=1
1739 GOTO 1699
1736 STOP
```

END

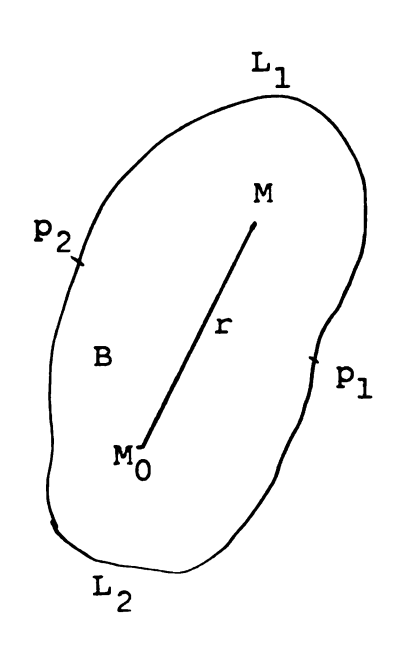
```
PROGRAM NEWPOSN
110
     FORMAT (4E14.8)
122
     FORMAT(2X, E14.8)
123
     FORMAT(2X, E14.8, 2X, E14.8)
124
     FORMAT (9X, 1HY, 15X, 1HX/)
125
     FORMAT(18X,E14.8,9X,E14.8)
 126 FORMAT(1HX)
     DIMENSION Y(21), X(21), PSI(21), XPRIM (21), YPRIM (21), XBAR(100)
     DELS=0.0
     DO 99 JBAR=100,900,100
     DO 96 I=1,24
  96 READ 126
     READ 110, XBAR (JBAR)
99
     DO 98 IBAR=1,9
98
     READ 122, PSI(IBAR)
     DO 60 I=1,8
     JBAR=1*100
60
     X(I+1) = XBAR(JBAR)
     X(1) = 0.0
     Y(1) = 0.0
     DO 70 I=1,9
70
     Y(I+1)=Y(I)+0.1
     DELTT=10.0
     DO 25 I=1,9
     IF(I-1)27,26,27
26
     DELX=X(I+1)-X(I)
     DELY=Y(I+1)-Y(I)
     DEPSI=PSI(I+1)-PSI(I)
     GOTO 80
261
     DY=DELY/DELS
     DX=DFLX/DELS
     DPSI=DEPSI/DELS
     GOTO 24
27
     IF(I - 9)29,28,29
28
     DELX=X(I)-X(I-1)
     DELY=Y(I)-Y(I-1)
     DEPSI=PSI(I)-PSI(I-1)
     GOTO 80
29
     DELX=X(I+1)-X(I-1)
     DELY=Y(I+1)-Y(I-1)
     DEPSI=PSI(I+1)-PSI(I-1)
     GOTO 80
30
     DELS=SQRTF(DELX*DFLX+DELY*DELY)
     GOTO 261
24
     FACTR=DY/30.
     DPSI=DPSI*4.0/(3.1415926
                                   *3.1415926
                                                )
     DELTY=(DPSI+FACTR)*DX*DELTT
     DELTX = (DPSI+FACTR)*DY*DELTT
     YPRIM(I)=Y(I)-DELTY
25
     XPRIi^{\dagger}(I) = X(I) + DELTX
     DO 97 I=1.9
97
     PUNCH 125, YPRIM(I), XPRIM(I)
     END
```

APPENDIX V

GREEN'S FUNCTION FOR LAPLACE'S EQUATION AND POISSON'S EQUATION

A. Definition*

In the mixed boundary-value problem, let the boundary L of the region B be separated into two parts,



L₁ and L₂, and let it be required to find in B a harmonic function u satisfying on the boundary L the conditions:

$$u = f_1(M)$$
 on L_1 ,

$$\frac{\partial u}{\partial n} = f_2(M)$$
 on L_2 .

The solution to this problem can be reduced to finding some singular particular

solution of the problem, which will be called Green's function for the mixed problem in the region B with pole at $M_0(x_0, y_0)$ and denoted by $G_g(x,y; x_0,y_0) = G_g(x,y)$.

^{*}The discussion in part A is abridged from L. V. Kantorovich and V. I. Krylov, Approximate Methods of Higher Analysis, 1952.

The Green's function is defined by the following requirements:

- 1. For each fixed point $M_0(x_0,y_0)$ in B, $G_g(x,y)$ as a function of x and y must be harmonic in B, with the exception of the point M_0 .
- 2. In the neighborhood of the point M_0 , $G_g(x,y)$ must have the representation:

$$G_g(x,y) = \frac{1}{2\pi} \ln \frac{1}{r} + h(x,y),$$

where $r = \sqrt{(x - x_0)^2 + (y - y_0)^2}$ is the distance between the variable point M and the pole M_0 , and h(x,y) is a function harmonic everywhere in B including even the point M_0 .

On the contour L of region B, G_g(x,y) satisfies the boundary conditions

$$G_{\alpha}(x,y) = 0 \text{ on } L_1$$

and

$$\frac{\partial}{\partial n} G_{\mathbf{g}}(\mathbf{x}, \mathbf{y}) = 0 \text{ on } \mathbf{L}_2.$$

If the Green's formula* is applied, we have

$$\int_{L} \left(u \frac{\partial^{G} g}{\partial n} - G_{g} \frac{\partial u}{\partial n} \right) ds + u(x_{0}, y_{0}) = 0.$$

From this, if we take into account the boundary conditions to which we have subjected $G_q(x,y)$, it will

^{*}Ibid., Equation (1), p. 480.

follow that

$$u(x_0,y_0) = -\int_{L_1} u \frac{\partial G_q}{\partial n} ds + \int_{L_2} G_q \frac{\partial u}{\partial n} ds,$$

and this last equation permits the computation of u at any interior point M_0 of the region if the Green's function $G_g(\mathbf{x},\mathbf{y})$ is known everywhere in B, and the values of u and $\frac{\partial u}{\partial n}$ are known on L_1 and L_2 , respectively.

For the problem with the rectangular region, we find the solution of the Poisson equation

$$\nabla^2 u = f(x,y)$$

with the boundary conditions

$$u = 0$$
 for $y = 0$, $y = d$

$$\frac{\partial \mathbf{u}}{\partial \mathbf{x}} = 0$$
 for $\mathbf{x} = 0$, $\mathbf{x} = \mathbf{b}$.

Let us now seek by Fourier's method* the fundamental function of the equation

$$\nabla^2 u = \lambda u.$$

Then we have

$$u_{m,n}(x,y) = \cos \frac{n\pi x}{b} \sin \frac{m\pi y}{d}$$

and

$$\lambda = -\pi^2 \left(\frac{n^2}{n^2} + \frac{m^2}{d^2} \right)$$
.

^{*}Ibid., pp. 69-71.

The function f(x,y) can be expanded in a double Fourier series,

$$f(x,y) = \sum_{m=1}^{\infty} \sum_{n=0}^{\infty} (\cos \frac{n\pi x}{b} \sin \frac{m\pi y}{d}) a_{m,n}$$

where

$$a_{m,n} = \frac{4}{bd} \int_0^b \int_0^d f(\xi, \gamma) \sin \frac{m\pi \gamma}{d} \cos \frac{n\pi \xi}{b} d\xi d\gamma.$$

The solution u can then be stated* thus:

$$u(x,y) = -\sum_{m=1}^{\infty} \sum_{n=0}^{\infty} \frac{a_{m,n}}{\pi^2(\frac{n^2}{b^2} + \frac{m^2}{d^2})} \sin \frac{m\pi y}{d} \cos \frac{n\pi x}{b}.$$

On substituting in the above equation the expression for $a_{m,n}$, we obtain

$$u(\mathbf{x},\mathbf{y}) = -\sum_{m=0}^{\infty} \sum_{n=0}^{\infty} \frac{4}{\pi^2 b d} \frac{\cos \frac{n\pi \mathbf{x}}{b} \sin \frac{m\pi \mathbf{y}}{d}}{(\frac{n^2}{b^2} + \frac{m^2}{d^2})} \int_{0}^{b} \int_{0}^{d} f(\mathbf{x}, \mathbf{y}) \cdot \cos \frac{n\pi \mathbf{x}}{b} \sin \frac{m\pi \mathbf{y}}{d} d\mathbf{x} d\mathbf{y}$$

$$= \int_{0}^{b} \int_{0}^{d} \left[-\frac{4}{\pi^2 b d} \sum_{m=0}^{\infty} \sum_{n=0}^{\infty} \cdot \frac{1}{\pi^2 b d} \sum_{m=0}^{\infty} \sum_{n=0}^{\infty} \cdot \frac{1}{\pi^2 b d} \sum_{m=0}^{\infty} \frac{m\pi \mathbf{y}}{d} \right] f(\mathbf{x}, \mathbf{y}) d\mathbf{x} d\mathbf{y}.$$

If the function of four variables in the square bracket be considered separately,

^{*}Ibid., p. 69.

$$G(x,y; \xi, \eta) = -\frac{4}{\pi^2 \text{bd}} \sum_{m=0}^{\infty} \sum_{n=0}^{\infty}$$
.

$$\frac{\cos \frac{n\pi x}{b} \sin \frac{m\pi y}{d} \cos \frac{n\pi \xi}{b} \sin \frac{m\pi \eta}{d}}{\frac{n^2}{b^2} + \frac{m^2}{d^2}}$$

by means of this function the solution of the problem can be very simply expressed:

$$u(\mathbf{x},\mathbf{y}) = \int_0^b \int_0^d G(\mathbf{x},\mathbf{y}; \, \mathbf{x}, \, \mathbf{y}) f(\mathbf{x}, \, \mathbf{y}) d\mathbf{x} d\mathbf{y}.$$

The function $G(x,y; \xi, \gamma)$ is the Green's function for a rectangle.*

B. Application to the Problem of Chapter III

In the problem of Chapter III, the boundary portion L_1 consists of the top and bottom of the rectangle of Figure 11, and the equation is Laplace's equation instead of Poisson's equation, so that the right-hand side f(x,y) is zero everywhere except at points on the interface. Since the interface is a line of sources, we have in effect taken it as the limiting case of a narrow zone, say of uniform width w on which $f(\xi, \gamma) = \frac{f(\xi, \gamma)}{w}$ where $f(\xi, \gamma)$ is the source strength. Then the area integral

^{*}See pp. 384-86 in R. Courant and D. Hilbert, Methods of Mathematical Physics, Vol. I, Interscience Publishers, New York, 1953.

$$\iint_{\text{Area of } G(\mathbf{x}, \mathbf{y}; \mathbf{x}, \mathbf{y}) f(\mathbf{x}, \mathbf{y}) dA}$$
Zone

becomes the line integral

$$\int_{\text{Interface}} \left[G(\mathbf{x}, \mathbf{y}; \mathbf{x}, \mathbf{\gamma}) - \frac{(\mathbf{x}, \mathbf{y})}{\mathbf{w}} \right] (\mathbf{w} ds)$$

which in the limit (as w approaches zero) reduces to the line integral

$$G(x,y; \xi, \gamma) \rho(\xi, \gamma) ds$$

to which must be added the integral along BA of Figure 11, the portion of L_2 where the normal derivative is prescribed to be different from zero. The remaining part of the integrals along L_1 and L_2 will be zero in this case because of the boundary conditions on Ψ .

Another way of looking at the problem is to note that each term of the series of Equation (50) satisfies Laplace's equation. Hence the series should satisfy Laplace's equation at interior points not on the interface, if it converges sufficiently. Each term of the series also satisfies the homogeneous boundary conditions. It remains only to show that the whole series satisfies the inhomogeneous boundary condition $\Psi_{\mathbf{X}} = -\mathbf{k}'$ on BA and the prescribed discontinuity condition on the interface.

Since the Green's function is the sum of $\frac{1}{2\pi} \ln \frac{1}{r}$ and a function h(x,y) harmonic in the whole rectangle, the required normal derivative discontinuity can only be furnished by the logarithmic term. What we have to show in order to justify Equation (47) is that

$$f(x,y) = \int_0^B \frac{1}{2\pi} \ln \frac{1}{r} \int (\xi, \gamma) ds - k' \int_B^A (\frac{1}{2\pi} \ln \frac{1}{r}) dy$$

has the prescribed normal derivative discontinuity, a jump of $\rho(\xi,\gamma)$ on DB and a jump of -k' across BA.

This can be shown from the potential theory* which states that the potential of a simple distribution on a curve

$$f(x,y) = \int_C \sqrt[r]{\ln \frac{1}{r}} ds$$

if the curve has a continuously turning tangent and \mathcal{X} is bounded and integrable, is continuous for all finite points of the plane including passage through C. If C has continuous curvature and \mathcal{X} is continuous, then the normal derivatives of f approach limits when P approaches A on C from either the positive or negative side, which satisfy the equations

$$\frac{1}{2}\left(\frac{\partial f_{+}}{\partial n_{A}} - \frac{\partial f_{-}}{\partial n_{A}} = -\pi \right)_{A}$$

where A is point on the curve C.

From this relation,

$$\frac{\partial f_2}{\partial n_1} - \frac{\partial f_1}{\partial n_1} = -2\pi (\frac{\gamma}{2\pi}) = -\gamma$$

which is the required jump condition for f(x,y) along DB or BA.

^{*}Quoted from W. J. Sternberg and T. L. Smith, The Theory of Potential and Spherical Harmonics, University of Toronto Press, 1944.

